HEALTH SCIENCES

Jarno Rieppo

Microscopic and Spectroscopic Analysis of Immature and Mature Articular Cartilage

Publications of the University of Eastern Finland
Dissertations in Health Sciences

UNIVERSITY OF EASTERN FINLAND

JARNO RIEPPO

Microscopic and Spectroscopic Analysis of Immature and Mature Articular Cartilage

To be presented by permission of the Faculty of Health Sciences of the University of Eastern Finland for public examination in Auditorium L22, Snellmania building, on Friday 11th March 2011, at one o´clock p.m.

Publications of the University of Eastern Finland
Dissertation in Health Sciences
41

Department of Anatomy, Institute of Biomedicine
School of Medicine, Faculty of Health Sciences
University of Eastern Finland, Kuopio Campus

Kuopio 2011

Kopijyvä Oy
Kuopio, 2011

Distribution:

Eastern Finland University Library / Sales of Publications
P.O. Box 1627, FI-70211 Kuopio, Finland
http://www.uef.fi/kirjasto

ISBN: 978-952-61-0355-6 (print)
ISBN: 978-952-61-0356-3 (pdf)
ISSN: 1798-5706 (print)
ISSN: 1798-5714 (pdf)
ISSNL: 1798-5706

Author´s address: Institute of Biomedicine, Anatomy
University of Eastern Finland, Kuopio Campus
P.O. Box 1627
FI-70211 Kuopio
FINLAND

Supervisors: Professor Heikki J. Helminen, M.D., Ph.D.
Institute of Biomedicine, Anatomy
University of Eastern Finland

Professor Jukka S. Jurvelin, Ph.D.
Department of Applied Physics
University of Eastern Finland

Reviewers: Professor László Módis
Department of Anatomy, Histology and
Embryology, Medical Faculty
University of Debrecen
Debrecen, Hungary

Professor Juha Tuukkanen
Department of Anatomy and Cell Biology
Institute of Biomedicine, University of Oulu
Oulu, Finland

Opponent: Professor Nancy Pleshko, Ph.D.
Department of Mechanical Engineering
Temple University
Philadelphia, PA
USA

Rieppo, Jarno. Microscopic and Spectroscopic Analysis of Immature and Mature Articular Cartilage. Publications of the University of Eastern Finland. Dissertations in Health Sciences 41. 2011. 101 pp.

ABSTRACT

Osteoarthritis (OA) is the most common joint disease affecting most people over 65 years of age. In spite of intensive research work, many aspects of the biology of articular cartilage and the pathogenesis of OA have remained unknown. The postnatal development of articular cartilage has been inadequately characterized. In particular, it has been proved challenging to characterize the architecture of collagen network and compositional changes in the tissue with imaging techniques. Thus one goal of this thesis was to develop further the methodological aspects of polarized light microscopy and Fourier transform infrared imaging spectroscopy (FT-IRIS) for use in cartilage research. This thesis work demonstrated that modern quantitative microscopy is able to measure local tissue changes that cannot be revealed with traditional biochemical techniques. When combined, polarized light microscopy and FT-IRIS provide a method for detailed characterization of collagen network architecture and volumetric changes in the amount of collagen. In particular, FT-IRIS holds a major potential for producing image maps of articular cartilage composition. However, further parameter development will have to be undertaken to increase the specificity of the FT-IRIS - derived proteoglycan and collagen parameters. The results also demonstrate that the collagen network undergoes significant postnatal modifications. This is a further support for the concept that the quality of articular cartilage can be affected by physical exercise in childhood.

National library of Medicine classification: WE 348
Medical subject headings: Articular cartilage; Microscopy; Spectroscopy; Collagen; Biomechanics

Rieppo, Jarno. Nivelruston kollageenisäikeistössä tapahtuvat muutokset kasvun aikana: Mikroskooppinen ja spektroskooppinen tarkastelu. Itä-Suomen yliopiston julkaisuja. Terveystieteiden tiedekunnan väitöskirjat 41. 2011. 101 s.

TIIVISTELMÄ

Nivelrikon kehittymiseen johtavat syyt ovat vielä pitkälti tuntemattomia. Nivelruston rakenne muuttuu suuresti nuoruusiän aikana. Kasvun aikaista kehitystä koskeva tietomme rajoittuu lähinnä nivelruston biokemiallisessa koostumuksessa tapahtuviin muutoksiin. Nivelruston kollageeniverkoston rakenteellisia muutoksia ei ole tutkittu riittävästi. Rakennetutkimusta on hankaloittanut käytettävissä olevien tutkimusmenetelmien rajoitteet. Väitöskirjatyön tavoitteena oli kehittää kollageenisäikeistön kuvantamiseen soveltuvien polarisaatiomikroskopian ja infrapunaspektroskopian menetelmiä rustotutkimuksen haasteita paremmin vastaaviksi. Väitöskirjatyössä osoitimme, että kvantitatiivinen mikroskopia näyttää luotettavasti ruston hienorakenteessa tapahtuvat paikalliset muutokset syntymän jälkeen ja yksilön kehityksen aikana. Polarisaatiomikroskopia ja infrapunaspektroskopia soveltuvat erityisen hyvin kollageenisäikeistössä tapahtuvien rakenteellisten ja määrällisen muutosten osoittamiseen. Infrapunaspektroskopia tarjoaa myös ainutlaatuisen mahdollisuuden muodostaa kuvakarttoja soluväliaineen koostumuksesta. Menetelmä mahdollistaa täysin uudenlaisten tutkimusten suorittamisen. Menetelmän kudosspesifisyys on kuitenkin vielä puutteellinen ja siten menetelmän jatkuva kehittäminen on välttämätöntä. Väitöskirjassa havaittu kollageenisäikeistön uudelleenjärjestäytyminen tukee aikaisemmin esitettyä hypoteesia lapsuusajan liikunnan mahdollisesta nivelrikkoa suojaavasta vaikutuksesta.

Luokitus: WE 348
Yleinen suomalainen asiasanasto (YSA): Nivelrusto; Mikroskopia; Spektroskopia; Biomekaniikka

To Niina, Janina, Eerika and Tuomas

Acknowledgements

Sometimes the journey itself becomes more important than the destination. This study was carried out during the years of 1998-2010 in the Institute of Biomedicine, Anatomy, University of Eastern Finland (formerly known as the Department of Anatomy, University of Kuopio).

I have been privileged to work under the supervision of Professor Heikki J. Helminen, M.D., Ph.D. He has had the patience to look after and to support my endless experiments and new ideas that have led (finally) to the completion of this thesis. His fatherly support and encouragement have been invaluable. I have been fortunate to have had a supervisor who has allowed me to follow my own path.

I owe my deepest gratitude to my supervisor Professor Jukka S. Jurvelin, Ph.D., who has shared his support and knowledge about cartilage research in general. His professional expertise in cartilage research has set high standards for us to strive for.

I want to express my most sincere thanks to Mika Hyttinen, M.D., who guided and taught me the secrets of quantitative microscopy. His support and long stimulating discussions have given me the ideas to further develop polarized light microscopy and Fourier transform infrared imaging.

Professors Markku Tammi, M.D., Ph.D., and Mikko Lammi, Ph.D., were my first mentors and they introduced me to the world of scientific work. I am greatly indebted to them for teaching me about biochemical and cell cultural research techniques.

I offer my deepest thanks to the official pre-examiners Professors László Módis and Juha Tuukkanen, for their constructive criticism and suggestions for improving the thesis.

Research work is seldom carried out by just a single independent researcher. I have been fortunate to be part of the Biophysics of Bone and Cartilage group of the Department of Applied Physics. I have been inspired by the hard work of young researchers and the efficient work of members of the

BBC-group. They all have set the goal high and it has been a really tough task to keep up with their pace. I want to offer my most cordial thanks to all members of the BBC group for their endless assistance whenever it was needed. My special thanks go to Professors Juha Töyräs, Ph.D., and Miika Nieminen, Ph.D. We started this journey together a long time ago and it has been a pleasure to follow the progress of their careers. All "graduated" members of BBC-group have provided a good example how hard work leads to its own rewards. You all are acknowledged.

I want to offer a very special thanks to my younger brother Lassi Rieppo, M.Sc., for his significant contribution to developing further the spectroscopic techniques. Our long telephone conversations have led to many new research ideas.

I want to express my gratitude for all co-authors. I am grateful to Jarmo Hallikainen, Ph.D., for his help in customizing the polarized light microscope. Customization would not have been possible without the technical expertise of Mr. Jukka Laakkonen from the Department of Applied Physics. Dr. Esa Halmesmäki, M.D., Henri Ruotsalainen, Ph.D., Jaakko Holopainen, M.D., and Panu Kiviranta M.D., Ph.D., offered assistance in the making of microscopic measurements and this is greatly appreciated.

I owe my deep gratitude to Docent Vuokko Kovanen, Ph.D., for performing biochemical analysis of the collagen and the cross-link contents. I also want to thank Professor Ilkka Kiviranta, M.D., Ph.D., and Dr. Anna Vasara, M.D., Ph.D., for the fruitful collaboration.

I want to offer cordial thanks to the whole personnel of the Department of Anatomy. I have received so much help from all of these skilled persons. I am especially thankful for the technical help given by Ms. Eija Rahunen and Mr. Kari Kotikumpu for preparing the histological sections used in the studies.

I am grateful for the financial support from the Ministry of Education, Academy of Finland, the National Graduate School of Musculo-Skeletal Diseases, the North-Savo Fund of the

Finnish Cultural Foundation, Intrumentarium Science Foundation, Finnish Medical Foundation, Duodecim Society, and Orion Pharma.

I offer my most sincere thanks to my parents Aimo and Arja Rieppo, as well as to my other relatives, for their continuous support and encouragement throughout my life.

Finally, I am grateful for having a family that has made all this meaningful. This research work would not have been possible without the full support from my beloved wife Niina and without the laughter and tears of our children Janina, Eerika and Tuomas. You have shown me what is significant and meaningful in life.

Kuopio, the 31st of January 2011

Jarno Rieppo

Original Publications

This thesis is based on the following original articles, which are referred to in the text by their Roman numerals:

I **Rieppo J, Töyräs J, Nieminen MT, Kovanen V, Hyttinen MM, Korhonen RK, Jurvelin JS, Helminen HJ:** Structure-function relationships in enzymatically modified articular cartilage. Cells Tissues Organs 2003; 175(3): 121-32.

II **Rieppo J, Hyttinen MM, Jurvelin JS, Helminen HJ:** Reference sample method reduces the error caused by variable cryosection thickness in Fourier transform infrared imaging. Applied Spectroscopy 2004; 58(1): 137-40.

III **Rieppo J, Hallikainen J, Jurvelin JS, Kiviranta I, Helminen HJ, Hyttinen MM:** Practical considerations in the use of polarized light microscopy in the analysis of the collagen network in articular cartilage. Microscopy Research Technique 2008; 71(4): 279-87.

IV **Rieppo J, Hyttinen MM, Halmesmaki E, Ruotsalainen H, Vasara A, Kiviranta I, Jurvelin JS, Helminen HJ:** Changes in spatial collagen content and collagen network architecture in porcine articular cartilage during growth and maturation. Osteoarthritis Cartilage 2009; 17(4):448-55.

This thesis also contains unpublished data related to articles II, III and IV.

Contents

Abbreviations

cm^{-1}	wavenumber, wavelength of the IR radiation
CCD	charge-coupled device
Da	Dalton, unit of molecular mass
ECM	extracellular matrix
FCD	fixed charge density
FTIR	Fourier transform infrared spectroscopy
FT-IRIS	Fourier transform infrared imaging spectroscopy
GAG	glycosaminoglycan
IR	infrared energy
MRI	magnetic resonance imaging
OA	osteoarthrosis, osteoarthritis
O.C.T.	embedding media used for cutting cryosections
PG	proteoglycan
PLM	polarized light microscopy
PLS	partial least square fitting, a data analysis method used for spectral analysis

Symbols

a	Indenter radius or microscope specific constant
b	microscope specific constant
c	concentration
l	optical path length
n_α	refractive index of fast axis
n_γ	refractive index of slow axis
p	statistical significance
A	amplitude, absorption
B	birefringence
E_{eq}	Young's modulus at equilibrium
I	intensity of emerging light
I_0	intensity of light illuminating the sample
$I_{(0\text{-}90^o)}$	intensity of light with polarizer at position 0-90º

M	molarity
$S_{0\text{-}3}$	Stokes parameters (4) that characterize the polarized state of light
T_2	spin-spin relaxation time, imaging modality in MRI
α	rotation angle of the polarization plane
α-axis	maximal light velocity for anisotropic material, fast axis
γ-axis	minimal light velocity for anisotropic material, slow axis
ε	molar absorptivity constant
θ	phase angle
κ	scale factor due to finite cartilage thickness
λ	wavelength
ν	frequency or Poisson's ratio
π	mathematical constant
Γ	optical retardation
ψ	orientation angle of polarization ellipse

1 Introduction

The degenerative joint disease, osteoarthrosis (or osteoarthritis, OA), represents a major financial burden in all developed societies (Altman 2010). In 1992 the annual economical costs were estimated at 64.8 billion dollars in the United States (Yelin and Callahan 1995). It has been estimated that OA affected 26.9 millions people in the the United States alone in 2005 (Altman 2010, Helmick *et al.* 2008, Lawrence *et al.* 2008). The aging of the population will increase the prevalence of OA in the near future. The appearance of OA symptoms increases dramatically between 40 and 50 years of age, particularly among women (Lawrence *et al.* 2008). OA causes pain, limitations in physical function, is a financial burden and the disease is one of the leading causes of premature retirement.

The pathophysiology of OA is not clear and this is probably one reason why there is no curative treatment for OA at the moment. Attempts at pharmacological intervention to slow down OA progression or even reverse the process have been made. Nowadays non-pharmacological therapies are regarded as the "cornerstone of OA management" and pharmacological interventions can be regarded only as add-on therapies. The non-pharmacological therapies can be divided into educational approaches and physical activities. Both aim at permanent lifestyle changes such as controlled diet and increased exercise. Instead, the pharmacological interventions mainly aim at reducing pain and discomfort. In addition, slower acting pharmacological options (intra-articular hyaluronate, oral glucosamine sulphate and chondroitin sulphate) have been used. Disease-modifying pharamacological therapies have failed to demonstrate significant effects and therefore pharmacological treatment is mainly regarded as symptom-relief instead of being curative.

Today, our understanding of the cartilage maturation process is far from complete. Cartilage tissue undergoes significant postnatal development and modification before the final phenotype of articular cartilage is reached. It is likely that the postnatal development is not a random event but rather a highly controlled process that attempts to produce the optimal tissue capable of withstanding the forces and wear caused by normal locomotion. It has been speculated that early juvenile loading conditions might be essential for the development of good quality articular cartilage.

The extracellular matrix (ECM) of articular cartilage is anisotropic and it cannot be fully characterized with traditional biochemical techniques. The spatial distribution of the tissue components and tissue architecture can only be captured with modern imaging methods. The main aim of this thesis was to further develop the existing quantitative imaging techniques (polarized light microscopy, PLM, and Fourier transform infrared imaging spectroscopy, FT-IRIS) to help in the characterization of the material properties of articular cartilage. These techniques were applied to characterize both the developing and the mature articular cartilage. Imaging techniques provided an effective way to investigate properties of the collagen network. The spatial distribution of collagen content and the collagen network architecture were evaluated with the techniques. This provides a basis for future studies aiming to characterize the development of articular cartilage and to study the pathophysiological mechanisms involved in OA.

2 Review of the literature

2.1 ARTICULAR CARTILAGE

2.1.1 Proteoglycans

Proteoglycans (PGs) are a class of glycoproteins that contain a central core protein to which one or more covalently linked glycosaminoglycan (GAG) side chains are attached. PGs can be divided into two categories: (1) aggregate-forming large PGs (aggrecan in cartilage) and (2) non-aggregating small PGs (decorin, biglycan, lumican and fibromodulin in cartilage). PGs account for 1/3 of the dry weight of the extracellular matrix of articular cartilage (Muir 1980). A concentration gradient with an increase of PGs can be seen from superficial to deep cartilage (Jones *et al.* 1977, Ratcliffe *et al.* 1984, Venn & Maroudas 1977). Aggrecan consists of up to 85% of the total amount of PGs in cartilage (Martel-Pelletier *et al.* 2008). Aggrecan has a unique ability to interact with hyaluronan. Its core-protein forms a non-covalent link with hyaluronan (Knudson & Knudson 2001). The linkage is further stabilized with a special link-protein (Hardingham 1979). A single hyaluronan molecule can bind over 100 PG subunits leading to the formation of a very large PG aggregate with a molecular mass of up to 10^8-10^9 Da (Dudhia 2005). Purified preparations of PG subunits (2.5×10^6 Da) contain 87% of chondroitin sulphate, 6% keratan sulphate and 7% of protein core (Hascall & Sajdera 1970). High amounts of negatively charged sulphate groups of GAGs lead to high fixed charge density (FCD) in cartilage tissue (Maroudas 1968). The FCD is able to create a high osmotic pressure in the tissue. PGs are bound to the ECM. The osmotic imbalance between articular cartilage and the surrounding tissue environment attracts cationic ions and water and creates a swelling pressure in cartilage.

The non-aggregating small PGs have been shown to be important during chondrogenesis and also in adult cartilage for maintaining and controlling ECM homeostasis (Knudson & Knudson 2001, Martel-Pelletier *et al.* 2008). However, the precise functional role of the small PGs has remained unclear. Decorin and lumican are associated with collagen fibrils (Martel-Pelletier *et al.* 2008). The interactions between the small PGs and collagen fibrils have been related to the control of collagen fibril diameter and fibril-to-fibril interactions (Martel-Pelletier *et al.* 2008). The surface decorating small PGs have also been proposed to limit the enzymatic cleavage of collagen fibrils and, therefore, be able to prevent the fibril damage (Geng *et al.* 2006).

2.1.2 Collagens

Collagen is the main macromolecular component of articular cartilage accounting for 2/3 of the dry weight of cartilage tissue (Martel-Pelletier *et al.* 2008, Muir 1980). Cartilage tissue contains several collagen types. Fibrillar type II collagen is characteristic of articular cartilage and it forms up to 90-95% of the total amount of collagen in cartilage (Eyre *et al.* 1992, Mayne 1989). Other collagens are found in articular cartilage *e.g.* types I, III, VI, IX, X, and XI (Eyre 2002, Eyre *et al.* 1992, Martel-Pelletier *et al.* 2008). However, these collagen types account for only 5-10% of the total amount of collagen in cartilage tissue (Eyre *et al.* 1992, Mayne 1989).

Type II collagen is a triple-helical fibrillar protein. Three identical α1(II) peptide chains intertwine for most of their lengths to create collagen molecules. Collagen fibrils are formed by the lateral and parallel association of collagen molecules. The adjacent molecules are linked together by either enzymatic pyridinoline or non-enzymatic glycation cross-links (Eyre *et al.* 1992, Fujimoto 1980). The non-helical telopeptide part of the collagen molecule is linked to the helical portion of the neighbouring collagen molecule. Hydrogen bonds and inter- and intramolecular cross-links stabilize the collagen fibrils and

prevent their thermal, chemical and mechanical degradation and provide high tensile stiffness for the fibrils.

The diameter of type II collagen fibrils of cartilage varies between animal species. The thickness of collagen fibrils varies also in the different zones of articular cartilage. In general, diameter of the collagen fibrils increases from the superficial zone toward the deep cartilage (Paukkonen & Helminen 1987). The fibril diameter has been reported to vary from 5nm to 200nm depending of the animal species and site of the measurement (Meachim & Stockwell 1979). The thinnest fibrils are found in the pericellular matrix, while the territorial fibrils are thicker with the thickest fibrils being found in the interterritiorial matrix (Meachim & Stockwell 1979). The highest collagen contents are found in the superficial tissue where it accounts for about 60-90% of the dry weight of the cartilage tissue (Venn & Maroudas 1977).

2.1.3 Histological structure

Articular cartilage is a specialized connective tissue that provides a wear-resistant and nearly frictionless protective cover between the bone ends of the diarthrodial joint. Articular cartilage is aneural, alymphatic, and avascular tissue (Meachim & Stockwell 1979). Cartilage distributes loads between the articulating bone ends onto a larger surface area. The main function of the tissue is to withstand the high loads and shear stresses generated during normal locomotion. The thickness of articular cartilage varies from some micrometers to a few millimetres depending on the animal species, the joint in question and the topographical location within the joint (Meachim & Stockwell 1979). Articular cartilage can be considered to consist of three components: (1) water, (2) extracellular matrix (ECM) and (3) cells, *i.e.* chondrocytes. The majority of the tissue wet weight (60-80%) is made up of water (Muir 1980). Articular cartilage contains also non-collagenous proteins and lipids in small quantities (Heinegård & Pimental

1992, Muir 1980). The chondrocytes produce ECM components and are responsible for its remodelling and maintenance during growth, maturation and adaptation of the tissue to joint loading. The cells occupy only 1-10% of the tissue volume. The cell density displays marked variations during the maturation of the tissue (Jadin *et al.* 2005). Also the density, shape and functional properties of the cells vary in the different zones of articular cartilage tissue (Jadin *et al.* 2005).

Collagen fibrils form a 3-dimensional network in articular cartilage. Superficial collagen fibrils are aligned parallel to each other and also run parallel with the surface. In the middle zone, collagen fibrils arch from the tangential to radial orientation in respect to cartilage surface and momentarily the parallel arrangement of the collagen fibrils is lost. In the deep zone of articular cartilage, the collagen fibrils run perpendicular to, *i.e.* at right angles with, the cartilage surface and show a high degree of organization. This pattern of collagen arrangement was first described in the 1920´s (Benninghoff 1925).

The zonal characterization of the cartilage tissue can be made according to the collagen fibril orientation and arrangement, the form of the chondrocytes, or the distribution of the PGs (Benninghoff 1925, Meachim & Stockwell 1979). The articular cartilage zones can be characterized as follows (Figure 1):

Zone I: Superficial or tangential zone, superficial layer of cartilage tissue adjacent to the joint cavity. The superficial zone occupies 5-10% of the cartilage thickness. Collagen content is high in the superficial tissue whereas the PG content is very low. Collagen fibrils are densely packed lying parallel to each other. Cells are small and discoidal. First tissue changes that predispose articular cartilage to OA, *i.e.* collagen fibrillation and loss of PGs, occur most often in the superficial zone (Freeman & Meachim 1979).

Zone II: Intermediate or middle zone, thickness of the zone varies depending on the method used to measure its thickness. It can occupy even 45% of the total thickness, if the cell morphology is used as the basis of the definition. However, the zone thickness can be less than 5% when the measurement is

based on polarized light microscopy investigation. The organization of the collagen fibrils is disturbed in the intermediate zone when fibrils arch from the tangential to the radial orientation. PG content increases in the intermediate zone. Chondrocytes become rounded and are evenly distributed in the tissue.

Zone III: Deep Zone, it occupies 45-85% of the tissue thickness. Collagen fibrils run at right angles (perpendicularly or radially) with the cartilage surface and are highly organized. PG content is highest in the deep cartilage. Cells are large and rounded, often arranged in columns that are aligned along with the collagen fibrils. Microstructure of the ECM can be divided into pericellular, territorial and interterritorial matrix (Meachim & Stockwell 1979).

Zone IV: Calcified zone; the "tidemark" serves as the demarcation line that separates the uncalcified and calcified cartilage tissues from each other. The calcified zone is adjacent to the subchondral bone. Its ECM is calcified and PG content low. The calcified zone contains only few chondrocytes. The cells are metabolically inactive and can show signs of degradation.

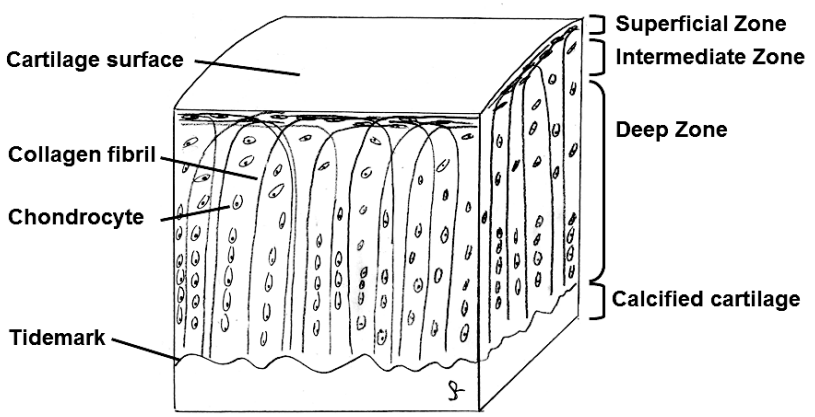

Figure 1. A schematic representation of the structure of articular cartilage. Collagen fibrils create a highly organized 3-dimensional network that entraps the PGs and chondrocytes within the cartilage. Uncalcified cartilage tissue can be divided into three different zones on the basis of the collagen fibril architecture. Superficial cartilage is

characterized by the presence of densely packed collagen fibrils that run parallel with the surface. Collagen fibrils arch from the parallel to the radial orientation in the intermediate zone where the orderly collagen fibril arrangement is momentarily lost. Collagen fibrils are strictly organized in the deep zone and the preferential orientation of the collagen fibrils is perpendicular to the cartilage surface. The amount of PGs increases from the superficial to the deep cartilage. Cells (chondrocytes) are sparsely distributed within the cartilage tissue. Cells have a columnar arrangement in the deep zone. The tidemark is the junction between the uncalcified and calcified cartilage tissue.

2.1.4 Biomechanical properties

The main function of articular cartilage is to reduce and redistribute stresses generated between the articulating bone ends. Furthermore, cartilage provides a surface with low friction to allow gliding motion of contacting bones. Normal biomechanical properties of articular cartilage must be maintained throughout the lifetime of the individual, because the tissue has a limited capability to repair any structural damage. Material strength and tensile stiffness of the cartilage tissue are greatly dependent on the properties of the fibrillar collagen network (Bae *et al.* 2008). The collagen network creates a framework for cartilage tissue and is able to resist tissue deformations, especially in the direction of the fibrils (Bae *et al.* 2008). Large PG aggregates are entrapped in the cartilage tissue and are immobilized due to their large size. Glycosaminoglycans (GAGs) of PGs are highly sulphated molecules and are, therefore, negatively charged (Muir 1980). The negative charges of GAGs generate an osmotic pressure that attracts free cationic ions and water into the cartilage (Maroudas 1968). Cartilage tissue swells to the point where the tensile stiffness of collagen network prevents further expansion of the tissue volume (Maroudas & Bannon 1981). The swelling pressure, generated mainly due to the sulphated GAGs of aggrecan, is needed to provide resistance against compressive loads.

Articular cartilage has unique biomechanical properties, being either nearly incompressible or highly compressible depending on the rate of loading. The mechanical properties are determined by the collagen content and the orientation of the fibrils as well as by the inhomogeneous distribution of PGs and water in ECM where water is pressurized, redistributed and squeezed out from the tissue as well as taken back during different loading conditions. The ability of water to move out and to be drawn back into the tissue is the key property of normal cartilage and it is thus which determines the functional quality of the tissue.

Articular cartilage can be considered incompressible when the load is applied very rapidly (Suh *et al.* 1995). Water is entrapped within the tissue during instantaneous loading (*e.g.*, during a heel strike during running). High hydrostatic pressure is generated within the tissue because the collagen network effectively prevents any change in the tissue volume. Collagen fibrils remain stretched and their high tensile stiffness withstands the generated load. On the other hand, cartilage tissue can be considered as relatively soft and compressible when the load is applied slowly, or kept constant over a period of time, *e.g.*, during standing. The articulating surfaces are in contact with each other. When the load is applied, hydrostatic pressure increases locally and water is gradually redistributed. Depending on the tissue permeability and loading, water is squeezed out and tissue deformation (compression) occurs. During compression, the contact area increases and the exposed load is applied onto a larger area than simply the initial contact area of the unloaded cartilage. The deformation ends when the osmotic swelling pressure in combination with intrinsic stiffness of the solid matrix achieves a balance with the applied load. At that time the cartilage is at mechanical equilibrium. After the load has been removed, the tissue becomes rehydrated to its original state due to the presence of the negative charges on the GAG molecules (Mow *et al.* 1990).

The biomechanical properties of articular cartilage can be determined using three different testing geometries: (1)

indentation, (2) unconfined compression, and (3) confined compression. Indentation requires minimal tissue preparation and is the only applicable testing method *in vivo.* In indentation testing, a local deformation of cartilage surface is produced with a plane-ended or spherical ended permeable or impermeable indenter. In the unconfined and confined compression tests, it is necessary to remove the cartilage specimen from the joint surface. Cylindrical cartilage samples are usually prepared for testing. The subchondral bone is detached before an unconfined test whereas a confined compression test may be carried out with osteochondral (cartilage-bone) samples. In unconfined compression, a cylindrical cartilage sample is placed between two smooth, frictionless and impermeable platens. When the load is applied, expansion of the tissue is allowed in lateral direction as the thickness of the tissue is decreased by compression. Water can escape through the lateral edges of the sample and thus the tissue volume decreases during tissue loading. In the confined compression test, lateral expansion of the sample is restricted as the sample is placed in a confined chamber having impermeable bottom and lateral walls. Then the water can only escape from the tissue through the permeable platen used for loading.

Mechanical loading can be applied by either using a constant displacement (stress-relaxation) or a constant applied load (creep-test). In the stress-relaxation test, multiple, small constant compression ramps are often performed. Initially, during compression, loading force rises rapidly to its peak value because no (or little) volumetric change occurs. The tissue response in this phase is highly related to the properties of the collagen network. After the loading ramp approaches its end, the measured force starts to decrease. Water flows out and the volume of the sample is reduced. Water flow is controlled primarily by permeability (controlled by PGs and collagen) and by the osmotic pressure of the sample (PG content). In the creep test, a constant force is applied onto the cartilage and the time-dependent deformation of the tissue is recorded until the equilibrium is reached.

All of the testing methods have their advantages and limitations. The indentation test mimics most closely the physiological loading conditions, but calculation of the results is complicated and may require utilization of sophisticated theoretical or mathematical models. The conditions during unconfined and confined tests are not physiological because special specimen preparation is needed. The unconfined test is two-dimensional since both axial and lateral strains occur simultaneously. The data from unconfined tests are easier to interpret than the indentation results. Sophisticated models are available for calculation of the biomechanical properties of collagen network, PGs and permeability. The confined compression test is simpler than the unconfined compression test since it is a uniaxial method. Compression and water movement takes place only perpendicularly to the cartilage surface. The confined compression test is less dependent on the collagen fibril properties since only axial compression occurs in the test.

Although the structure and composition of the cartilage tissue determines the functional properties, the biomechanical behaviour of articular cartilage is highly complex and not fully understood. Therefore, studies addressing structure-function relationships of articular cartilage could be predicted to open new insights for tissue engineering experiments where artificial cartilage tissue is produced for cartilage repair purposes. Detailed spatial analyses of both the composition and the collagen network architecture provide means for developing realistic mathematical models of cartilage biomechanics. Sophisticated models can be used for simulation of different structural changes and their influence on biomechanical properties. This approach provides also a possibility to study the pathophysiological mechanisms of OA more efficiently.

2.2 DEVELOPMENT OF CARTILAGE

2.2.1 Collagen network

At birth, cartilage tissue lacks the highly anisotropic nature of collagen network found in mature cartilage (Clark *et al.* 1997, Schenk *et al.* 1986). The collagen fibrils are arranged randomly and distributed inhomogeneously in cartilage (Clark *et al.* 1997, Eikenberry *et al.* 1992). Biochemical studies have shown that the collagen content increases during tissue maturation (Klein *et al.* 2007, Williamson *et al.* 2001). At an early age, biochemical synthesis of collagen is active. Simultaneously, the amount of proteolytic enzymes in the ECM is high which suggests that postnatal modulation of the collagen network takes place in the cartilage (Brama *et al.* 2000, Brama *et al.* 1998, Brama *et al.* 2004). The solid matrix content of cartilage tissue increases gradually over time. The solid matrix accounts for only 12 % of the wet weight of fetal tissue. During maturation, the solid matrix of the tissue can increase up to 32% of the wet weight (Pal *et al.* 1981, Strider *et al.* 1975, Thonar & Sweet 1981). Mostly, the increase of the solid content is related to the collagen content, and it has been reported to more than triplicate during maturation (Klein *et al.* 2007).

The increase in collagen content has been proposed to be related to a functional adaptation of the tissue on account of altered loading conditions (Brama *et al.* 2002, Brama *et al.* 2000). After birth, different regions of the joint exhibit very similar biomechanical properties and composition that markedly differ from those of mature animals (Brama *et al.* 2002, Brama *et al.* 2000). Changes in the tissue composition can be observed within a few months after birth (Brama *et al.* 2002, Clark *et al.* 1997). In human cartilage, biochemical modulation of the collagen network, including cross-linking of the fibrils, gradually generates the mature fibril network at about the age of 20 years (Bank *et al.* 1998). This indicates that structural modification of the collagen network is declining and the final phenotype of collagen network has been reached. It is likely that in addition to

changes due to growth and maturation, the gradual compositional changes reflect the adaptation to different functional requirements at different joints and joint locations. During growth and maturation, the formation of enzymatically generated pyridinoline cross-links significantly alters the mechanical properties of collagen network. Non-enzymatic glycation end products, such as pentosidine, start to accumulate in cartilage linearly with time after 20 years of life. Interestingly, this has been speculated to be a potential cause for the development of OA (Bank *et al.* 1998).

Initially, the diameter of collagen fibrils is rather constant in different zones and sites of articular cartilage tissue. During maturation, the fibril diameter starts to change spatially in different depths of ECM and in various joint areas. The superficial tissue contains thin (20nm) fibrils whereas thicker (200nm) fibrils are found in deep cartilage (Hunziker *et al.* 1997, Meachim & Stockwell 1979). In addition, pericellular, territorial and interterritorial matrices show differences in collagen fibril thickness (Hunziker *et al.* 1997, Meachim & Stockwell 1979, Paukkonen & Helminen 1987).

The architecture of the collagen network also undergoes changes during maturation (Nakano *et al.* 1978, van Turnhout *et al.* 2010a, Wei *et al.* 1998) In particular, recent histomorphometric and magnetic resonance imaging studies have pointed to significant maturation dependent alterations in the collagen network (Grunder 2006, Hunziker *et al.* 2007), leading to the hypothesis that the original collagen network is being gradually degraded. This is followed by the formation of new collagen fibrils with new qualities and a distinct organization. The mature cartilage bears only a slight similarity with the fetal collagen network architecture (Grunder 2006, Hunziker *et al.* 2007). Hunziker et al. (2007) related the significant remodelling of articular cartilage to its role as a kind of growth plate of the bone end during postnatal development (Carlson *et al.* 1985, Hunziker *et al.* 2007). The epiphysis undergoes rapid enlargement. The joint is mostly enlarged by lateral expansion of the articular surface. Therefore, the collagen network runs

predominantly in parallel with the surface during the initial phase of remodelling (Hunziker *et al.* 2007). As the growth of the joint slows down, the second phase of the remodelling begins in the perpendicular direction (Hunziker *et al.* 2007). This hypothesis of cartilage maturation is primarily based on observations of cell morphology and rearrangement of the chondrocytes in the deep tissue according to the collagen fibril orientation. However, no direct quantitative measurements on collagen fibril orientation or spatial changes of collagen content were provided in that report (Hunziker *et al.* 2007).

MRI studies of T_2-relaxation support the remodelling theory. The T_2 mapping can be used to measure properties of collagen network due to the angular dependence of collagen fibril orientation in reference to a static magnetic field (Erickson *et al.* 1993, Nieminen *et al.* 2001, Xia *et al.* 2003). The T_2-imaging of mature cartilage tissue reveals a tri-laminar appearance (Rubenstein *et al.* 1993). Further, T_2-measurements have indicated an even higher number of layers or laminas in cartilage (Grunder *et al.* 2000, Nieminen *et al.* 2001, Nissi *et al.* 2006, Xia 2000, Xia *et al.* 2003). This multilaminar appearance has been suggested to reflect the maturation and growth of the cartilage (Nieminen *et al.* 2001). Using T_2-measurements, the orientation and organization of the collagen fibrils have been shown to change during maturation of both animal and human cartrilage (Grunder 2006, Nissi *et al.* 2006, Xia *et al.* 2003). Recently, the gradual modulation of collagen network during maturation, revealed systematic changes in the appearance of laminar structures which were demonstrated by T_2 images of cartilage (Hannila *et al.* 2009). Although the MRI findings have given some insight into the level of the tissue microstructure, there have been only a few attempts with other imaging techniques to systematically characterize the spatial changes of collagen content, fibril orientation and organization (Kiviranta *et al.* 2006, van Turnhout *et al.* 2010b, van Turnhout *et al.* 2010a, Xia *et al.* 2002, Xia *et al.* 2001). In fact most of the knowledge has emerged from the biochemical data on spatial compositional

differences, collected from layered cartilage slices (Bank *et al.* 1998, Klein *et al.* 2007).

2.2.2 Changes in proteoglycan content

Characteristically, adult articular cartilage shows inhomogeneous distribution of PGs from the cartilage surface to deep tissue. However, this depth-wise pattern of PG content is not evident during the fetal period (Thonar & Sweet 1981). The PG content of articular cartilage also depends on whether the measurements are normalized against wet or dry weight of the tissue, respectively (Maroudas *et al.* 1973). This can be explained by the lower water content of the mature in comparison with young and immature tissue (Brama *et al.* 2000, Maroudas *et al.* 1973). Not only does the PG content change during maturation but the magnitude of the change is also different in different joints and joint regions (Brama *et al.* 2000). In horses, during the fetal period and at birth, there is no topographical variation of the average PG content when different regions of the joint are analyzed (Brama *et al.* 2000). Topographical variations in PG concentration start to take place within the first 5 months after birth (Brama *et al.* 2000). Overall the detected PG changes are less dramatic than the changes observed in collagen content during the maturation (Williamson *et al.* 2001).

In adult individuals and during aging, PGs can experience extensive post-translational modifications. In particular, glycosylation and sulphatation of the GAG chains and core proteins can show significant modifications. The GAG changes include an increase in the amount of keratan sulphate and a decrease in that of chondroitin sulphate during aging (Bayliss & Ali 1978, Bjelle 1975, Venn & Maroudas 1977). Chondroitin and keratan sulphate chain lengths decrease and increase, respectively (Brown *et al.* 1998, Santer *et al.* 1982). These modulations have been reported to control the size and composition of the aggregating PGs (Mitchell & Hardingham 1982). Furthermore, selective enzymatic modification of core proteins of PGs also occurs during aging. This enzymatic

degradation results in the accumulation of partially degraded aggrecan molecules in ECM (Dudhia 2005). Link protein production decreases when the individual reaches skeletal maturity (Bolton *et al.* 1999). This leads to a relative deficiency of link protein and may produce weaker PG aggregates (Tang *et al.* 1996).

2.2.3 Changes in biomechanical properties

The extensive changes in the tissue structure and composition that occur during maturation evoke significant alterations in the biomechanical properties of the cartilage. A significant increase of tensile stiffness has been reported during the early period of the development (Kempson 1991, Kempson 1982, Roth & Mow 1980, Williamson *et al.* 2003, Williamson *et al.* 2003). Fetal bovine cartilage shows very low tensile stiffness but during postnatal development, stiffness increases by over 1000% (Williamson *et al.* 2003). In humans, the tensile strength of the superficial tissue increases from 5 MPa to 10 MPa between 8 to 20 (-30) years of age. Thereafter, there is a gradual decline in the tensile stiffness with time (Kempson 1982). Tensile stiffness of the immature cartilage increases with depth and reaches the maximum value at the cartilage-bone junction (Roth & Mow 1980). Mature tissue shows an opposite behaviour the superficial tissue layer, having the maximum stiffness and the deeper tissue being less stiff (Roth & Mow 1980). The observed changes have been proposed to follow from the increased collagen and cross-link content in the superficial tissue (Williamson *et al.* 2003, Williamson *et al.* 2003).

During growth and maturation, significant alterations occur in the compressive properties of cartilage. The mean aggregate modulus has been reported to increase by 180% from the fetal period to adult age (estimated by unconfined compression equilibrium stress-strain data (a mathematical approximation) (Williamson *et al.* 2001). Simultaneously, the permeability of the tissue was reported to decrease by 70 % (Williamson *et al.* 2001). The changes were claimed to be due to increased collagen

content and not to differences in PG content. Most of the detected changes occurred during the first phase of maturation, thereafter only smaller changes were detected (Williamson *et al.* 2001). The instantaneous response to rapid compression, *i.e.* instantaneous modulus, has also been reported to decrease with age (Wei *et al.* 1998). A reduction in the instantaneous modulus was observed during early maturation, after which the modulus no longer changed (Wei *et al.* 1998). The change was proposed to reflect the altered organization of collagen network (Wei *et al.* 1998). Recent experimental and modelling results on the maturation of rabbit cartilage have pointed to similar findings (Julkunen *et al.* 2009). Specifically, the compressive equilibrium stiffness and the non-fibrillar matrix equilibrium modulus, calculated by fibril-reinforced poroelastic finite element model, increase during maturation. This was thought to be related to an increase in the tissue PG content during maturation. The instantaneous modulus, which depends primarily on the collagen content, increased during the first six weeks of maturation in the rabbit but decreased during later periods of life (Julkunen *et al.* 2009).

2.2.4 Functional adaptation

Both biochemical and biomechanical properties display significant alterations during tissue maturation. It is reasonable to assume that to a large extent, the detected changes are related to the altered loading conditions of the joints, reflecting functional adaptation of articular cartilage. It has been proposed that physical exercise in childhood and adolescence can improve the properties of articular cartilage and even postpone or prevent the OA changes of the tissue in later life (Helminen *et al.* 2000). There are several studies indicating that the level of physical exercise or the absence of the exercise affects the quality of articular cartilage (Arokoski *et al.* 1994, Arokoski *et al.* 1993, Brama *et al.* 2001, Brama *et al.* 2000, Brommer *et al.* 2005, Jortikka *et al.* 1997, van Weeren *et al.* 2008). The type and the level of the exercise affect the quality of articular cartilage in

different ways. Immobilization (no exercise) has been shown to cause long lasting changes in the PG content of articular cartilage. Immobilization of the beagle knee joint for 11 weeks evoked a decrease in the amount of PGs that were not completely restored during 50 weeks of remobilization (Haapala *et al.* 1999, Jortikka *et al.* 1997). Moderate exercise is believed to be beneficial for developing articular cartilage. Treadmill running of young beagles (4 km/h day, five days a week for 15 weeks) increased the thickness and PG content of femoral condylar cartilage but no changes were detected in the amount of collagen (Kiviranta *et al.* 1988). In addition, a statistically significant stiffening of the articular cartilage (+6% compared to controls) was observed to take place after the same exercise regimen (Jurvelin *et al.* 1986). Instead, strenuous exercise has been reported to lead to an inferior quality of the tissue (Arokoski *et al.* 1994, Arokoski *et al.* 1993, van Weeren *et al.* 2008). In conclusion, articular cartilage is a dynamic tissue during growth and maturation, but the fully mature tissue maintains its highly unique structure with only minor modifications (DeGroot *et al.* 2001, Maroudas *et al.* 1992, Verzijl *et al.* 2000). It is clear that characterization of the features of normal maturation process and improved knowledge of the effects of exercise on cartilage would be important in clarifying the development of the adult articular cartilage.

2.3 OSTEOARTHROSIS (OA)

OA is a degenerative joint disease which leads to a gradual degradation of the cartilage tissue and impaired function of the joint (Buckwalter & Martin 1995). Even today, the pathophysiological mechanisms leading to OA are unclear. OA has multiple etiologies but all seem to include the contributions of mechanical factors (Radin 1998). The risk factors of the OA are age, overweight, injuries, manual labour, sports and genetic factors (Arokoski *et al.* 2007). Superficial fibrillation of the collagen network takes place during the normal ageing process

and, therefore, this change cannot be considered as a hallmark sign of OA (Freeman & Meachim 1979). Vertical clefts are a pathological change and they result in thinning of the cartilage layer (Freeman & Meachim 1979). The first signs of OA include the loss of PGs in the superficial cartilage tissue accompanied by fibrillation of the superficial tissue collagen network. Cell death and remodelling of the subchondral bone accompany these initial changes (Freeman & Meachim 1979, Radin *et al.* 1970). In the later stages of OA, the water contents of the cartilage increase, causing the thickness of the tissue first to increase and later to become reduced (Bank *et al.* 2000, Freeman & Meachim 1979). Age-related superficial fibrillation (non-destructive) and osteoarthritic collagen network degradation (destructive) result in a variety of different morphological features, suggesting that there are different pathophysiological mechanisms behind the changes observed (Freeman & Meachim 1979).

Articular cartilage has only a limited capability to heal after an injury (Buckwalter & Mankin 1997). The OA process triggers a mechanism in which both synthesis and degradation of ECM molecules takes place (Buckwalter & Mankin 1997). Failure of the repair mechanisms ultimately leads to increased cell death, cloning of chondrocytes, and both mechanical and biochemical degradation of the cartilage tissue (Buckwalter & Mankin 1997, Freeman & Meachim 1979).

The early stages of OA are asymptomatic and the structural damage may accumulate over a long period of time. An increase in pain and impaired joint mobility are the clinical signs of the OA process (Buckwalter & Martin 1995). Early symptoms of OA typically fluctuate, *e.g*. pain and joint stiffness can disappear for a period of time but the pathophysiological changes continue unaltered. Eventually, some kind of analgesic medication is needed and the patient starts to suffer pain also at rest. Already at an asymptomatic stage of OA, irreversible structural changes have taken place in cartilage. Surgical treatments of OA include osteotomy, allogenic or autologous grafts, autologous chondrocyte transplantation, debridement of the joint and penetration of subchondral bone (Newman 1998). Although

novel repair methods have been devised, the outcome of the interventions varies from patient to patient. Tissue engineering approaches have not yet fulfilled their initial promise. Despite active research work and major investments, at present there is no artificial cartilage tissue that possesses the same kind of functional properties as normal healthy cartilage (Service 2008).

Currently, the general practice treatment of OA is mainly based on clinical findings and symptoms together with radiological findings of the joint (Arokoski *et al.* 2007). Initially, the OA treatment is based on the reduction of pain and discomfort together with recommendations concerning weight loss, diet and exercise (Arokoski *et al.* 2007). Acetaminophen (with a dose up to 3g/day) is used for primary pain relief. Non-steroidal anti-inflammatory drugs are also used for managing pain but their use is secondary not primary, since these compounds increase the risk of the gastrointestinal side-effects (ulcer and gastrointestinal-bleeding) and pose an increased risk of experiencing cardiovascular events (Berenbaum 2008). Surgical interventions may be considered when the patient is suffering pain also at rest even when treated with drugs. The four generally used surgical approaches are osteotomy (for young patients), mosaicplasty (transplantation of autologous cartilage-bone grafts from non-weighbearing areas to the injured site) (Hangody & Fules 2003), autologous chondrocyte implantation (Brittberg *et al.* 1994) and total joint replacement arthroplasty (Arokoski *et al.* 2007). In the future, treatment of young OA patients may change when cartilage repair techniques develop.

2.4 POLARIZED LIGHT MICROSCOPY

2.4.1 Theoretical basis of polarized light microscopy

The theoretical background of the polarized light microscopy (PLM) is based on an understanding of the electrical nature of matter and the wave nature of the light. A light transmitting

medium has a molecular and elemental structure where electrons of the medium interact with oscillating light waves. When light passes through an elastic medium, its electric field vibrates in the transverse direction with a simultaneous vibration of the magnetic field that has an equal amplitude and coincident phase at right angles with the plane of oscillation of the electric component (Bennett 1950, Collett 1992, Kliger & Lewis 1990, Modis 1991) (Figure 2**)**. The molecular nature of matter affects the penetration of light waves. This interaction can be utilized in PLM to obtain information about the structure and orientation of an object at the submicroscopic resolution level.

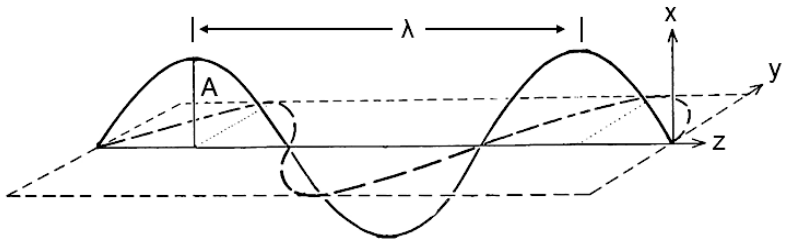

Figure 2. Schematic presentation of light propagation through an elastic medium. Oscillation has two components, electric and magnetic, oscillating at right angles with each other. The electric component (dotted line) lies in the y-plane and the magnetic vector (solid) oscillates in the x-plane. Both components have the same phase and their amplitude (A) follows a sine wave. Wavelength (λ) is indicated in the diagram.

An isotropic material has electronic resonators distributed perfectly randomly in a spherically symmetrical manner. Light passes through an isotropic material with equal velocity despite the state of the polarization or the course of the propagation. The light velocity change but there is no alteration in the polarization plane. Anisotropic materials transmit light differently in relation to the plane of polarization or the direction of propagation. When a material has more than one refractive index for a given frequency, the material is said to be birefringent or double refractive (Bennett 1950, Modis 1991). The birefringent nature of a material can be due to several reasons.

Asymmetric assignment of the chemical bonds, ions or molecules within a transmitting material can cause birefringence (*i.e.* intrinsic birefringence). Uniaxial bodies (*i.e.,* material where only one optical axis exists) display birefringence when the material is organized and surrounded with a medium that has a different refractive index (*i.e.,* form birefringence). An otherwise isotropic material can be made anisotropic by subjecting it to mechanical stress. Under stress, the molecular bonds can change their orientation and the material can become birefringent (*i.e.,* strain anisotropy). Some substances (sugars, amino acids) possess the ability to rotate the plane of polarization (*i.e.,* rotary birefringence) (Bennett 1950).

When incident light strikes an anisotropic material, the light beam splits into two linearly polarized coherent components with equal frequencies and amplitudes that oscillate perpendicularly to each other. One component has the maximum velocity (α-axis) and perpendicular to it lays the γ-axis that has a slower propagating velocity. These two components travel through the material at different velocities and, therefore, the slow (γ-axis) component is left behind. This difference is called optical retardation Γ. Retardation can also be regarded as a phase difference between the α-axis and γ-axis components. The phase angle or the phase difference is called θ. If only negligible dispersion occurs, then the retardation is constant for any given object but the phase difference varies with frequency. Retardation Γ and phase difference θ can be defined as follows:

$$\Gamma = l \times \left(n_\gamma - n_\alpha \right) \text{ or } \theta = \frac{l \times \left(n_\gamma - n_\alpha \right)}{\lambda} , \qquad (2.1)$$

where l=optical path length, n_γ=slow axis refractive index, n_α=fast axis refractive index, λ=wavelength.

Each wavelength has its own characteristic behaviour when travelling through a transmitting medium. It is impossible to calculate each and every wavelength since the phase term does

not cancel out in the equations. This obstacle can only be overcome by using a monochromatic light source. When a monochromatic light is used, the mathematical equations are simplified since the phase term is cancelled out and calculations become possible. This ground rule is strict and has to be borne in mind when quantitative calculations are being performed.

Birefringence is defined as an intrinsic property of a material independent of its thickness. Birefringence describes the medium property that is due to the asymmetric nature of the chemical structure. Birefringence (B) can be defined as a thickness-normalized value of the retardation as follows:

$$B = \frac{\alpha \times \lambda}{\pi \times l}\ , \tag{2.2}$$

where α=rotation angle of the polarization plane, λ=wavelength of the monochromatic light, l=optical path length and π is the mathematical constant.

In PLM, typically two linear polarizers are used. Non-polarized light is linearly polarized by the first polarizer. The second polarizer is rotated perpendicularly to the first one and therefore no light is allowed to go through the system when ideal polarization purity is reached. If an anisotropic material is placed between the polarizers, the polarization plane is rotated and some light will pass through the system. The degree of the rotation (the amount of detected light) depends on the intrinsic anisotropic nature of the material as well as on the form birefringence of the organized fibrillar or spherical material. In the case of two linear polarizers adjusted to be perpendicular to each other, the intensity of emerging light (I) can be related back to the degree of the rotation of the polarization plane using the Fresnel equation:

$$I = a + b \times I_o \sin^2 \alpha \, , \, 0 \leq \alpha \leq \pi/2 \, , \qquad (2.3)$$

where I_0 is the intensity of the light illuminating the sample, I is the intensity of emerging light, and a and b are constants specific for the optical system. If α is solved from equation 2.3 and placed into equation 2.2, which can then be written in the form:

$$B = \frac{\lambda}{\pi \times l} \arcsin \sqrt{\frac{I - a}{b \times I_0}} \qquad (2.4)$$

Traditional linearly polarized systems have significant limitations. The detected signal has angular dependence when uniaxial bodies (*e.g.,* long cylindrical samples such as collagen fibrils) are studied. All fibrils are not detected with equal sensitivity. The maximal signal is detected from superficial and deep fibrils of the sample when the cartilage surface is aligned at 45° angles with the polarizers. The sensitivity decreases gradually and when an oblique direction (45°) in the intermediate zone is approached, the sensitivity becomes zero (Figure 3). Linearly polarized systems cannot see the true signal from the sample since the analyzer plane (second polarizer) will restrict the wave oscillation.

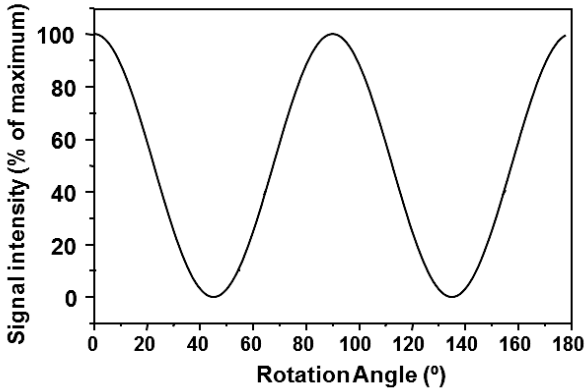

Figure 3. Schematic presentation of the detected signal intensity with linearly polarized light. A birefringent object is placed between the crossed polarizers (polarizer and analyser). The detected signal intensity fluctuates when the polarizer and analyser are rotated.

Maximal signal originating from the sample is only momentarily seen if the object is placed optimally in reference to the polarizers. With biological samples, this produces an underestimation of the actual birefringence level since a tissue sample cannot be placed optimally for every image element.

The full polarization phenomenon can be characterized mathematically with the so-called Stokes parameters (Collett 1992). The state of polarization can be completely described by four parameters that can be determined by measuring the light intensity at different polarizer settings. The first Stokes parameter expresses the total intensity of the optical field. The remaining three parameters describe the state of the polarization. The Stokes parameters can be described as follows:

$$S_0 = I_{(0^\circ)} + I_{(90^\circ)} \qquad S_0 = I_{(0^\circ)} - I_{(90^\circ)} \qquad (2.5)$$
$$S_2 = 2 \times I_{(45^\circ)} - S_0 \qquad S_3 = S_0 - I_{(90^\circ + \lambda/4 Phasesifter)}$$

where I=light intensity, S_0 = total intensity of light, S_1=the amount of linear/horizontal polarization, S_2=the amount of +45° or -45° polarization and S_3=the amount of right and left circular polarization. Intensity subscripts refer to background corrected 0°, 45°, 90° and the 90° images taken with the phase shifter.

2.4.2 Application of polarized light microscopy in cartilage research

Polarized light microscopy can be used to visualize and quantitatively characterize the properties of collagen network in articular cartilage (Adany *et al.* 1979, Arokoski *et al.* 1996, Kocsis *et al.* 1998, Ortmann 1975, Speer & Dahners 1979, Xia *et al.* 2003). When the crossed polarizers are coupled in series, no light is detected. When a thin transparent cartilage section is placed between the polarizers, the sample forces the polarization plane to rotate, and, thus some light passes through the sample and thus an image can be seen by aid of the oculars. The contrast of

the image is generated by the birefringent nature of the sample. The intensity of light seen in the image is related to the amount of optical activity of the sample.

PLM can be conducted using stained (Picrosirius Red or other topo-optical dyes) or untreated transparent samples. The Picrosirius Red F3BA molecule has been widely used for dyeing collagen (Constantine & Mowry 1968). The elongated stain molecule is aligned parallel with the collagen fibril. The presence of the stain molecule enhances significantly the anisotropy of collagen fibrils (Modis 1991, Puchtler *et al.* 1973). Staining was even proposed to be able to distinguish types I, II and III collagens from each other (Junqueira *et al.* 1978). Later, this finding proved to be incorrect and the staining differences were found to be related to the diameter of the collagen fibrils (Junqueira *et al.* 1982). In fact, it has been shown that the fibril staining differences cannot be explained by diameter alone (Dayan *et al.* 1989). Since Picrosirius staining is specific for collagen, it has been recommended for quantitative estimation of collagen content (Junquiera *et al.* 1979). However, the staining involves various unspecific interaction mechanisms and the dye binding has been shown to be non-stoichiometric. Therefore, it cannot be used for the quantitative determination of collagen (Puchtler *et al.* 1988).

Topo-optical enhancement of the collagen network birefringence is no longer needed in the era of modern CCD-camera technology. Transparent, untreated cartilage sections with weak birefringence can nonetheless be easily measured without any additional staining procedures (Arokoski *et al.* 1996, Király *et al.* 1997, Xia *et al.* 2001). Today, due to uncertainties inherent in the staining procedures, staining is no longer recommended. Unstained samples offer the best possibilities for determination of the birefringence of the cartilage tissue and other polarization derived parameters such as collagen fibril orientation.

The use of the traditional linearly polarized systems is restricted to visualization and qualitative investigation of collagen network. The manual use of rotatable compensators

makes it possible to gather quantitative information, but the measurements are laborious to perform (Bennett 1950). The use of the CCD camera technology has enabled an effective collection of quantitative information about the light intensity with the added possibility to conduct quantitative calculations over an entire image (Arokoski *et al.* 1996, Kocsis *et al.* 1998). As stated above, the quantitative PLM measurement is influenced by the orientation of the collagen fibrils in the tissue. The introduction of the liquid crystal compensator opened a new era of PLM (Oldenbourg 1996, Oldenbourg & Mei 1995). The universal compensator makes it possible to calculate the orientation independent birefringence and the orientation of the fibrillar structures via the Stokes calculus. This innovation has increased significantly the possibilities to use PLM in the quantitative characterization of the collagen network. It solved the problem associated with the angular sensitivity of the measured material and made feasible the measurement of true retardation values. Further technical advancements have been introduced into cartilage research to characterize the collagen network in a more optimal manner (Alhadlaq & Xia 2004, Xia *et al.* 2002, Xia *et al.* 2003, Xia *et al.* 2001).

2.5 FOURIER TRANSFORM INFRARED IMAGING SPECTROSCOPY

2.5.1 Theoretical basis of Fourier transform infrared spectroscopy

Fourier transform infrared spectroscopy (FTIR) is one of the most widely used and versatile techniques for the analysis of the chemical composition of solids, liquids or gases. Infrared spectrometers have been commercially available already since the 1940s. In general, infrared energy interacts with the material and part of the energy is transmitted through the sample while part is lost via the vibration and the rotation of the intra- and intermolecular bonds within the specimen (Stuart 2004).

Normally, a broad band of infrared (IR)-energy will pass through the sample and the fraction of the absorbed energy is determined for each wavelength. The peaks of the absorption spectra can be related to a specific interaction of the IR-energy and the molecular structure of the sample (Figure 4).

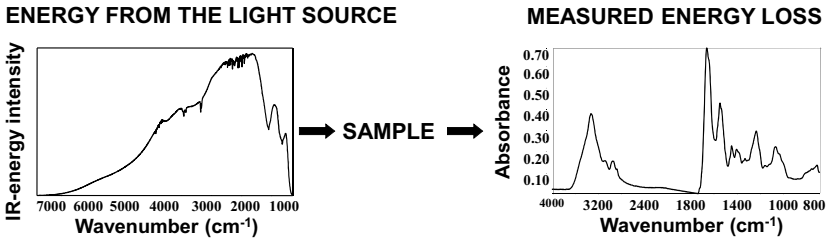

Figure 4. Simplified presentation of principles of the Fourier transform infrared spectroscopy. The spectrometer has an infrared source that emits a known amount of energy. Emitted infrared energy is transmitted through the sample. The amount of the energy absorbed by the sample is calculated for each frequency (or wavelength) separately and the results are plotted as a spectrum that characterizes the measured sample. The absorption peaks detected can be used to analyze the chemical composition of the studied material.

Each molecular bond has its own characteristic resonance frequency. Molecules can be described as masses linked together with bonds that have spring-like properties (Stuart 2004). When the broad band IR energy is introduced into the system, the intra- and intermolecular bonds start to resonate at their resonance frequencies and this causes the absorption of IR energy (Stuart 2004). Each of the molecular bonds has its own characteristic resonance frequency that is determined by the type of bond (single, double or triple bond) and the type of molecule (diatomic or polyatomic and linear- or non-linear molecule). The characteristic frequency is also affected by the stiffness of bond and the masses of the atoms at each end of the bond (Stuart 2004).

Molecular vibrations can involve either a change in bond length (stretching) or bond angle (bending). Vibration can occur either in-phase (symmetric) or out-of-phase (asymmetric). Vibrations can occur in six different ways (Figure 5).

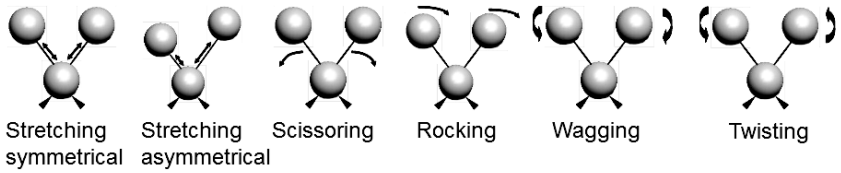

Figure 5. Schematic presentation of different possible infrared resonance modalities that occur at intra- and intermolecular chemical bonds. Infrared energy is absorbed and transformed into bond vibration. This is the fundamental principle behind the interpretation of the infrared absorption spectra.

The amount of IR-energy absorption is proportional to the change in the dipolar moment of the molecule (Stuart 2004). Therefore, FTIR is a very powerful tool for the characterization of polarized molecules, and only weak absorption is seen with unarranged linear molecules. If symmetrical stretching occurs in a linear molecule, the resulting IR absorption is low, but symmetrical molecules can also be IR-active if the type of vibration is asymmetric.

Individual molecular bonds absorb energy at their characteristic frequency. The measured FTIR spectrum is a sum of all of the theoretical bond vibrations within the studied material. Sharp, delineating peaks are only seen with simple materials. The peaks may widen not only due to the material properties but also because of the technical issues related to the instrumentation. For example, complex molecules may have the same bonds in different regions of the molecule and individual vibrations from different parts of the molecule can be coupled. Coupling commonly occurs at C-C stretching, C-O stretching, C-N stretching, C-H rocking and C-H wagging motions (Stuart 2004). In coupling, the energy levels of the bond vibrations with similar frequencies are mixed, particularly when the bonds are close together in the same part of the molecule. Coupling restrains the linkage between the detected absorption peaks to distinct bonds in specific locations of the molecule. Coupled skeletal vibrations of a complete molecule can contribute to the measured FTIR spectrum as a whole rather than via a specific group within the molecule (Stuart 2004).

Protein spectroscopy is demanding since all of the proteins are built from the same amino acids. The protein spectrum is usually divided into nine different regions: Amide A, B and I-VII in a decreasing order of wavenumber. The characteristic infrared amide absorption bands are presented in Table 1. The relative proportions of different amino acids, secondary and tertiary structure of the proteins and cross-linking of the proteins and their side chain substitutions are the main sources of the differences detected between different biological tissues. The composition of the sample introduces variation into the absorption peak frequencies (*e.g.* the peak shift phenomenon). Most of the structural information of the proteins is obtained from wavenumbers in the range 1500-600 cm^{-1}, known as the fingerprint region. Each individual pure compound has its own absorption pattern (chemical fingerprint) that is unique for that material. Due to the molecular similarities between different tissues, the exact molecular composition of complex tissues cannot be analyzed directly from the measured IR spectra. Each tissue component contributes to the measured spectrum but the sub-components of the spectra are summed together and seen as a single spectrum.

Table 1. Characteristic infrared bands seen in protein spectroscopy. Infrared absorption arises from the intra- and intermolecular absorption of amino acids.

Designation	Wavenumber (cm^{-1})	Assignment
A	3300	N-H stretching in resonance with harmonic overtone of Amide II
B	3100	
I	1653	C=O stretching (80%), C-N stretching (10%), N-H bending (10%)
II	1567	N-H bending (60%), C-N stretching (40%)
III	1299	C-N stretching (30%), N-H bending (30%), C=O stretching (10%), O=C-N bending (10%), other vibrations (20%)
IV	627	O=C-N bending (40%), other vibrations (60%)
V	725	N-H bending
VI	600	C=O bending
VII	200	C-N torsion

The table is adapted from Stuart B: Infrared Spectroscopy: Fundamentals and Applications (Stuart 2004).

When mixtures of pure compounds or biological tissues are measured, the components might have interactions causing peak shifts. Therefore, the measured spectra might differ from the theoretical pure compound model. In theory, measured absorption levels obey the Beer-Lambert Law that relates the absorption (A) to the concentration as follows:

$$A(\overline{\upsilon}) = \varepsilon_{\upsilon} \times c \times l \,, \tag{2.6}$$

where ε is molar absorptivity constant of the material, c is concentration, υ is frequency (wavenumber) and l is the optical path length of the sample.

The measured absorption levels can be related to the amount of the studied substance, provided that the pure compound calibration is conducted with known concentrations. Quantitative measurements are easy to perform with pure compounds. However, for biological tissues, quantitative analysis is demanding since a specific part of the spectrum has to be isolated for each tissue component. Normally, one cannot conduct quantitative measurements, as derived from the IR spectrum without additional data analysis. Sophisticated analysis methods, such as curve-fitting, second derivative spectroscopy, principal component analysis, and other multivariate techniques have to be utilized in order to obtain specific quantitative sub-component information.

FTIR spectroscopy can also be used for studying qualitative material differences. Modern sophisticated mathematical tools have been introduced for dividing a collected dataset into smaller subsets that possess similar spectral features; a procedure called cluster analysis. This is solely done on the basis of spectral information and it can be conducted completely without any *a priori* information about the material in question (unsupervised method). Cluster analysis can also be applied for cartilage studies that only are interested in identifying qualitative characteristics of the tissue (*e.g.,* intact vs. OA tissue, intact vs. repair tissue, mature vs. immature tissue). Cluster

analysis techniques have been widely applied in bioscience, especially for cancer and microbiological diagnostics (Fabian *et al.* 2002, Fabian *et al.* 2006, Lasch *et al.* 2002, Lasch *et al.* 2007, Lasch *et al.* 2004, Sahu & Mordechai 2005).

2.5.2 Application of Fourier transform infrared spectroscopy in cartilage research

Since 2000, FTIR spectroscopy has been used in cartilage research. First, Camacho *et al.* (2001) and Potter *et al.* (2001) introduced a concept for analysing the biochemical composition of articular cartilage with Fourier transform imaging spectroscopy (FT-IRIS) (Camacho *et al.* 2001, Potter *et al.* 2001). The first studies utilized two alternative approaches for analyzing articular cartilage collagen and proteoglycan content. Camacho *et al.* (2001) applied a straightforward univariate method for quantitative determination of collagen and proteoglycan contents. The collagen and proteoglycan contents were determined by integrating the Amide I absorption area (1710-1595 cm^{-1} wavenumbers) and the carbohydrate area (1185-960 cm^{-1} wavenumbers), respectively (Camacho *et al.* 2001). Linear positive correlations were revealed between the FTIR parameters and the biochemical reference methods. Potter *et al.* (2001) introduced a more sophisticated multivariate approach for semiquantitative estimation of the relative contribution of collagen and PGs to the measured spectra (Potter *et al.* 2001). In this method one must have knowledge of the pure compound's spectral data and the so-called Euclidean distance. Furthermore, a least square fitting approach based on pure compound's spectra has to be used to calculate information about collagen and PG. The spatial distribution of collagen and PGs were calculated in both reports (Camacho *et al.* 2001, Potter *et al.* 2001). Later, the techniques were used to characterize OA changes in cartilage tissue (Bi *et al.* 2007, Bi *et al.* 2006, David-Vaudey *et al.* 2005, West *et al.* 2004, West *et al.* 2005). Compositional changes in OA (decreased collagen integrity and PG depletion) were detected with FTIR imaging studies and with an intra-articular

fibre-optic probe (Bi *et al.* 2007, West *et al.* 2004). FTIR-derived parameters were able to detect decreased PG and collagen contents as well as increased collagen degradation and altered collagen fibril orientation from a single FTIR measurement (Bi *et al.* 2006). All of the detected changes correlated well with the histological findings, thereby supporting the potential feasibility of this technique.

When the absorbance of a fibrillar sample has to be assessed, the IR measurement is affected by the polarization or circular dichroism (Coats *et al.* 2003). The orientation of the sample (*i.e.* the sample is rotated) affects the measured absorbance levels in a sample with anisotropic properties (aligned transitional moments along with the fibrillar structure). The intensities of Amide I, II and III peaks vary as the measurements are carried out using a linearly polarized system (Bi *et al.* 2005, Camacho *et al.* 2001, Ramakrishnan *et al.* 2008, Ramakrishnan *et al.* 2007, Xia *et al.* 2008, Xia *et al.* 2007). The sugar region (1200-1000cm^{-1} wavenumbers) is not affected by the polarization effect (Xia *et al.* 2007). The detected phenomenon can be explained by the fact that Amide I and Amide II molecular vibrations will exhibit a dichroism in a direction both parallel and perpendicular to the long axis of the triple-helix of the collagen molecule (Fraser & MacRae 1973). Molecular vibrations from C=O stretch (Amide I) and the combination of the C-N stretch and N-H bending vibrations (Amide II) have almost perpendicular transitional moments to each other (Bi *et al.* 2005, Xia *et al.* 2007). Sinusoidal fluctuation of the detected signal occurs when the plane of polarization is rotated and the peak intensities of Amide I and II peaks will be out of phase by ~ 90°. The detected maximum and minimum values have an angular deviation of 8-15 degrees from the orientation of cartilage surface (Bi *et al.* 2005, Xia *et al.* 2007). This offset is likely to be related to the biochemical properties of the collagen molecule even though the exact transitional moment angles of the Amide I and II are still unclear. In the case of cartilage, the sectioning plane also affects the anisotropic properties which are being detected. When sectioning is done perpendicularly to the cartilage surface, most

of the collagen fibrils will be sectioned along their long axis. When the sectioning plane is parallel with the surface, most of the collagen fibrils will have been cut perpendicularly to their long axis (cross-section). When sectioning is done along the long axis of the fibrils, both amide I and II have anisotropic properties (Amide I being more strongly influenced due to the stronger effect of the double bonds). However, when collagen fibril cross-sections are studied, only Amide I exhibits intense anisotropy because Amide II has almost no anisotropic features (Ramakrishnan *et al.* 2008).

The anisotropic properties of Amide I and II can be used to estimate collagen fibril orientation from a single measurement under linear polarizaton (Bi *et al.* 2005) or by doing multiple rotations of the polarization plane and the calculating the orientation (Xia *et al.* 2007). Methods have been devised to determine the zonal division of articular cartilage (Bi *et al.* 2005, Camacho *et al.* 2001, Ramakrishnan *et al.* 2007). One disadvantage of the polarization experiments, even when the partially polarized light is used, is that it affects the quantitative measurement of the collagen content (Coats *et al.* 2003). However, Amide I and II intensities have not been reported to change when the sample is rotated and no polarizer is used (Bi *et al.* 2005). One cannot achieve an unbiased estimation of the collagen content from straightforward measurements under polarized light condition, since cartilage has collagen fibrils oriented both parallel (surface) and perpendicular (deep tissue) to the cartilage surface. Since the intensity of Amide I peak shows orientational dependence, the intensities do not obey the classical Beer-Lambert's Law and the absorbance cannot be directly related to concentrations.

Successful measurement of collagen and PG contents in articular cartilage requires the application of analysis methods that are specific only for collagen or PGs. Since the pure compound spectra of collagen, aggrecan and chondroitin sulphate overlap strongly (Figure 6), there are no characteristic peaks for either collagen or PGs that can be used for simple unbiased determination of collagen or PG concentrations.

Previously, Amide I absorption (1710-1595 cm^{-1} wavenumbers) and carbohydrate area (1185-960 cm^{-1} wavenumbers) were used to analyze collagen and PG contents, respectively (Camacho *et al.* 2001). The theoretical specificity of Amide I for collagen alone is questionable when pure compound data is analysed. Though there is a distinct peak shift between the collagen and aggrecan Amide I peaks, this shift is too small to fully differentiate these two compounds from each other (Figure 6). Therefore, no specific determination of collagen or PGs can be made directly from the absorbance spectrum, even though there does exist a high correlation between the biochemical composition and the FTIR derived parameters exists (Camacho *et al.* 2001). Enzymatic removal of PGs can be used for enhancing the specificity for collagen (Laasanen *et al.* 2005). However, complete removal of PGs from mature tissue specimens is challenging, probably due to the non-enzymatic glycation of aggrecan (DeGroot *et al.* 2001). Enzymatic manipulation cannot be used for more specific determination of PGs, since collagen cannot be degraded without loss of PGs from tissue. The spectral area of 1200-900 cm^{-1} contains PG-related information, as demonstrated earlier (Camacho *et al.* 2001). However, collagen also absorbs in the same region which means that there will be overlapping spectral information about PGs and collagen (Figure 6). Therefore curve fitting or multivariate partial least square (PLS) models have to be utilized to derive more specific information on the PG concentration. The specificity of PG determination from articular cartilage was recently improved by using multiple curve fitting of the carbohydrate region (1100-900 cm^{-1}). A sub-peak, located at 1060 cm^{-1}, was found to be more specific for PGs than the previously utilized parameters (Rieppo *et al 2010a.*).

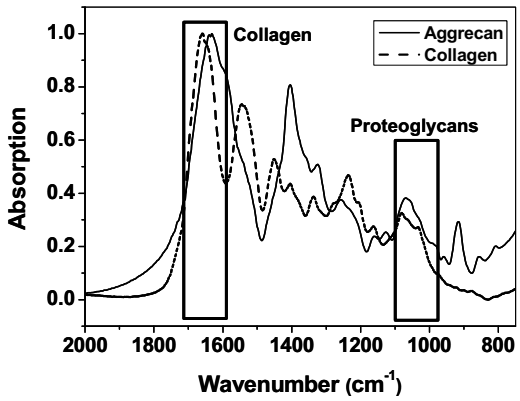

Figure 6. Pure compound spectra of purified bovine articular cartilage type II collagen and aggrecan. Collagen and aggrecan spectra are mutually overlapping and no specific peaks can be directly assigned to either collagen or proteoglycans. The spectral areas previously used for collagen and proteoglycan content measurements are highlighted in the figure.

Second derivative spectroscopy offers a possibility to analyse spectra more effectively. The second derivative spectrum displays negative peaks for the peaks and shoulder areas of the spectrum. Derivation dramatically increases the noise present in the spectrum and, therefore, data quality is an issue hindering successful analysis. Further, the measurement time increases as the repeated scans have to be averaged. The advantage of derivative spectroscopy is that peaks are significantly narrowed and the method can resolve additional peaks located within the original envelope spectrum. This allows isolation of small additional peaks and this provides increased tissue specificity. Second derivative analysis has been previously carried out for biological tissues (Belbachir *et al.* 2009, Kohler *et al.* 2007, Paschalis *et al.* 1997, Vesela *et al.* 2007). The previously reported second derivative peak assignments concerning collagen and PG molecules are listed in the Table 2.

FTIR measurements are affected also by non-chemical factors. Recently, scattering of IR-energy has been recognized to influence the recorded spectrum (Kohler *et al.* 2007, Kohler *et al.* 2005). Light scattering may affect quantitative measurements in various ways, *e.g.* causing baseline anomalies and the peak shift

phenomenon. The implications of scattering effects in quantitative cartilage measurements are currently unknown. However, it is evident that cartilage tissue is dense enough to cause scattering of IR-energy. Baseline anomalies are evident and most likely due to this scattering phenomenon. The density of the cartilage tissue varies because of the uneven distribution of collagen and PGs and, therefore, the magnitude of scattering might also vary according to tissue depth.

Table 2. Summary of the previously reported peak assignments of 2nd derivative protein spectroscopy studies. The most promising cartilage related areas are highlighted according preliminary findings from unpublished research projects (Närhi *et al.* 2010, Rieppo *et al.* 2010b).

Wavenumber (cm^{-1})	Assignment of second derivative peaks
1700-1600	Amide I region (C=O stretch)
1600-1500	Amide II region (C-N stretch + N-H bend)
1448	CH_3 asymmetric bending vibrations (Jackson *et al.* 1995, Kohler *et al.* 2007)
1400	COO^- stretch of amino side chains (Jackson *et al.* 1995)
1376	**CH_3 symmetric bending vibration of GAGs (Jackson *et al.* 1997)**
1336	**CH_2 side chain vibrations of collagen (Jackson *et al.* 1995)**
1280	Collagen amide III vibration with significant mixing with CH_2 wagging vibration from the glycine backbone and proline side chain (Jackson *et al.* 1995)
1228	SO_3^- asymmetric stretching vibration of sulfated GAGs (Servaty *et al.* 2001)
1200	**Collagen amide III vibration mixed with CH_2 wagging vibration from the glyine backbone and proline side chain (Jackson *et al.* 1995)**
1120	C-O-S asymmetric stretching (Servaty *et al.* 2001)
1080	C-O stretching vibrations of the carbohydrate residues in collagen and proteoglycans (Jackson *et al.* 1995, Kohler *et al.* 2007)
1060	**C-O stretching vibrations of the carbohydrate residues in proteoglycans (Jackson *et al.* 1995, Kohler *et al.* 2007) / SO_3^- symmetric stretching vibration of sulfated GAGs (Servaty *et al.* 2001)**
1032	C-O stretching vibrations of the carbohydrate residues in collagen and proteoglycans (Jackson *et al.* 1995, Kohler *et al.* 2007)

3 Aims of the study

The structure and composition of articular cartilage determines its unique functional properties, properties which are crucial for normal joint function. While biochemical methods are important they are unable to characterize the volumetric distribution profiles of tissue constituents. Quantitative imaging techniques are preferable when the structure-function relationships are to be studied in non-homogeneous cartilage. Polarized light microscopy has been used for visualization of the collagen network architecture. Fourier transform infrared imaging spectroscopy offers a tool for the determination and visualization of the biochemical composition of the cartilage tissue from histological samples. The main goal of this thesis work was the further development of the polarized light microscopy and the Fourier transform infrared imaging techniques for use in cartilage research, with a special emphasis on characterizing quantitatively structure, composition and function of cartilage using these techniques.

In this thesis work, the following specific aims were to:

- compare biochemical methods and quantitative microscopy for determination of the changes in tissue composition induced by enzymatic manipulation of articular cartilage,

- improve, by development of new instrumentation and software, the applicability of quantitative polarized light microscopy for the characterization of the collagen network in articular cartilage,

- explore and apply Fourier transform infrared imaging spectroscopy for qualitative and quantitative cartilage research,

- investigate structure-function relationships of articular cartilage after specific structural alterations,

- characterize the growth and maturation related changes of the collagen network in articular cartilage.

4 Materials and methods

This thesis study consists of four independent studies along with some unpublished data. Studies II and III address methodological development of Fourier transform infrared imaging and quantitative polarized light microscopy, respectively. Experimental work in cartilage biology plays a major role in studies I and IV. The unpublished information consists mostly of new FT-IRIS data.

4.1 SAMPLE PREPARATION

Bovine patellar cartilage, delivered from the local abattoir (Atria Oyj, Kuopio, Finland) within 2h *post mortem*, was used in studies I-III. Complete knee joints with intact joint capsules were derived from 1- to 3-year-old steers. Porcine cartilage samples from animals of different ages were used in study IV. Samples for light microscopy were prepared for studies I, III and IV. Fourier transform infrared imaging was performed in studies II, III and IV. Biomechanical testing and biochemical reference measurements for collagen and PG contents were conducted in study I.

Study I: Samples for these experiments were processed within a few hours *post mortem*. Cylindrical osteochondral samples were prepared from the lateral upper quadrant of patella using a hollow drill bit (dia.=13mm) and an autopsy saw (Stryker Autopsy Saw 868, Stryker Europe bv, Uden, The Netherlands). The underlying bone was trimmed using a diamond saw (Buehler Isomet Low Speed Saw, Buehler, Lake Buff, IL, USA). One to two mm of subchondral bone remained attached to the cartilage sample. The samples were kept moist at all times during preparation and only visually intact cartilage was used

in these studies. Samples were divided into five separate groups (control samples, n=24, and incubation group, n=12). Control samples were used for biomechanical testing immediately after preparation. The other samples were incubated at 37ºC for 44 h, in cell culture medium with antibiotics. The ECM components were degraded using spesific enzymes. The superficial collagen network was degraded using bacterial collagenase enzyme capable of cleaving collagen fibril at neutral pH (Shingleton *et al.* 1996). Chondroitinase ABC and elastase were used to deplete PGs (Mok *et al.* 1992, Yamagata *et al.* 1968). Human neutrophil elastase was chosen for the experiment in order to obtain more physiological PG degradation results. Human neutrophil elastase has been linked to cartilage destruction in rheumatoid arthritis (Cawston & Young 2010, Moore *et al.* 1999, Wang *et al.* 2004). Extra controls (n=12) were also incubated in cell culture medium with no additional enzymes. The incubation medium supplemented with enzymes was changed after 22h to ensure maximal enzyme activity. A smaller sample (dia.=9mm) was punched out from the center of the specimen after incubation and the peripheral rim of the sample was omitted to ensure that no lateral penetration of the enzyme occurred from the edges of the sample. The final sample for the biomechanical testing and microscopic evaluation was prepared by punching out a 6mm diameter sample with a steel punch. The adjacent surrounding tissue was used for biochemical measurements

Study II: Cartilage samples without subchondral bone (2x2 mm pieces) were prepared with a razor blade from the intact patella. Samples were embedded in Tissue-Tek O.C.T. cryogenic embedding medium immediately after the preparation. A piece of nitrocellulose western blotting membrane (Protran, Schleicher&Schuell, Keene, NH, USA) was first hydrated using 20% methanol and placed next to the cartilage samples. Using a cryomicrotome (Reichert-Jung Frigocut 2800, Nussloch, Germany), sections were cut from the frozen tissue block. Both the sample and the reference membrane were cut simultaneously and the sections were transferred from the

microtome knife to measuring windows (2-mm BaF_2-windows, Spectra-Tech, Madison, WI, USA). Five sections at three different nominal section thickness settings (5μm, 10μm, 14μm) were prepared. Samples were allowed to air-dry for one day prior to the measurements.

Study III: The samples originally prepared for studies I and IV were used. Additional samples from the cartilage repair study were used for illustrative purposes (Vasara *et al.* 2006). A microscopy slide with an air-bubble captured between a slide and a coverslip was also used for illustrative purposes.

Study IV: Porcine articular cartilage from the lateral facet of femoral trochlea was used. Three separate age groups were formed (4-, 11- and 21-month-old groups, N=12 in each). Samples were prepared immediately after the sacrifice of the animals and cartilage surface was kept moist continuously during the preparation. Cylindrical cartilage-bone samples were drilled and detached from the joints with the same technique as used in study I. The samples were fixed in formalin, decalcified and embedded in paraffin. Thin histological sections were prepared and processed for polarized light microscopy and FT-IRIS as described later (see 4.2.1 and 4.3).

4.2 PURE COMPOUND SAMPLES FOR FT-IRIS

Spectral information of purified bovine type II collagen and aggrecan was measured. Articular cartilage from the bovine femoral condyles was collected for preparation of the collagen and aggrecan. Cartilage was chopped into small pieces and PGs were extracted with 4 M guanidinium hydrochloride in 50 mM sodium acetate buffer (pH 5.8) supplemented with 10 mM disodium EDTA, 100 mM e-amino-n-caproic acid and 5 mM benzamidine at 4°C for 60 h. The extract was dialyzed against deionized water (Spectra/Por dialysis tubing, molecular weight cut-off 12,000-14,000, Spectrum Laboratories). Ethanol

precipitation (75% ethanol containing 0.3 M sodium acetate) of PGs was carried overnight at 4°C. Finally, the precipitate was washed with 70% ethanol. Residual tissue was washed with deionized water and digested with 0.05% pepsin (Sigma, St. Louis, MO, USA) in 0.5 M acetic acid for 24 h at 4°C. The released collagen was isolated using the NaCl precipitation method (Miller 1972).

4.3 LIGHT MICROSCOPY

4.3.1 Linearly polarized light microscopy (Studies I and III)

Traditional linear PLM setting was used in studies I and III (Arokoski *et al.* 1996). Four different tissues blocks, with randomized vertical orientation (sectioning planes) were prepared. Samples were fixed with formalin, decalcified, dehydrated in an increasing series of alcoholic solutions and finally embedded into paraffin (Paraplast Plus, Lancer Division of Sherwood medical, Kildare, Ireland) (Király *et al.* 1997). Multiple thin (5-µm-thick) transparent sections perpendicular to the cartilage surface were cut with a microtome (LKB 2218 HistoRange microtome, LKB produkter Ab, Bromma, Sweden). Sections were placed onto microscopy slides and deparaffinized with xylene. Sections were further treated with bovine testicular hyaluronidase (Sigma Chemical, St. Louis, MO, USA) at 37ºC for 18h to achieve enzymatic removal of PGs. After enzyme treatment, samples were dehydrated once in 70% alcohol and thereafter three times with absolute alcohol and finally mounted with DPX (Gurr, BDH Laboratory Supplies, Poole, England).

Linear PLM studies were performed using a Leitz Ortholux BK-2 polarized light microscope (Leitz, Wetzlar, Germany). The system was equipped with strain-free optics, two rotatable linear polarizators (polarizer-analyzer pair), $\lambda/4$-retardation plate, monochromator (λ=589±10nm) and a peltier-cooled 12-bit CCD-camera (Photometrics CH 250/A, Photometrics Inc., Tucson, AZ, USA).

Cartilage sections were placed between the linear polarizers and the cartilage surface was turned to a 45º position with reference to the plane of polarization. Two sets of images were captured using an objective x6.3 (pixel resolution 3.6 x 3.6μm). One image was taken and another captured when the crossed polarizers were turned 45º. Individual background images were also taken and subtracted from both images. The images were fused with an image analysis software using the max-function. The final image was formed pixel-by-pixel from the original two images by taking the larger greyscale value for each pixel. This was done to decrease the angular dependency of the detection sensitivity. After this procedure, the grey scale image was converted to the birefringence image using inverse Fresnel-equations described in section 2.4.1.

Three sections of each four tissue blocks were measured. A region of interest (ROI) 627μm wide was measured from each section. The measurements were conducted from the cartilage surface to cartilage-bone junction. The measured pixel values from ROI were averaged in the transversal direction and the depth-wise birefringence profiles were taken from each measured section. Finally, all independent 12 measurements were averaged and the averaged data-vector was used in the final calculations. The procedure ensured that variable section thickness and possible sectioning plane dependency did not affect the final calculations.

4.3.2 Enhanced polarized light microscopy (Studies III and IV)

Sample preparation for enhanced polarized light microscopy was identical to that of the above-mentioned traditional linear PLM. As compared to study I, the measurement system and measurement principle used for studies III and IV were further developed. The new system was a modified version of the Leitz Ortholux BK-2 polarized light microscope (Leitz, Wetzlar, Germany). Polarizers and $\lambda/4$-retardation plate were replaced by precision grade optical components (Precision linear polarizer, 10LP-VIS and 10RP34 phase shifter, Newport Corporation,

Irvine, CA, USA) and mounted in computer controlled high-speed rotation tables (PR50 high-speed rotation tables and ESP300 control unit, Newport Corporation, Irvine, CA, USA). The system was operated with an IpLab 3.5.5 software (Scanalytics Inc., Fairfax, VA, USA). The electrical supply (Mascott 9522, Mascot Electronics AS, Fredrikstad, Norway) and the monochromators of the system were also new (591.4±10nm, Schott, Germany, 594±3nm XLK10, Omega Optical, USA). The CCD camera was updated to a 12-bit peltier-cooled camera (Photometrics SenSys, Roper Scientific, Tucson, AZ, USA). After these modifications, the microscope was computer-controlled with 0.01° angular resolution of the polarizer positions.

In the updated system, automated alignment and calibration routines were run before the system was operated. The rotation table was aligned prior to the calibration routines. Calibration was performed by rotating the polarization plane at 0.1° steps and recording the light intensities. Calibration was done for each pixel element separately to avoid the potential bias generated by uneven illumination of the sample at the edges of the imaging area.

Multiple images were collected for final calculations. Images were recorded at 0°, 15°, 30°, 45°, 60°, 75°, 90° polarizer pair positions and an additional image was taken at the 90° position with $\lambda/4$-retardation plate in the light path. Background images were collected for each position separately and subtracted from the original images.

The system allowed the determination of the Stokes parameters, as described earlier in section 2.4.1. Birefringence could be calculated analogously to the traditional linearly polarized measurements using the inverse Fresnel equations. Enhanced polarized light microscope could be used to measure the true birefringence without variable angular sensitivity, an issue that can lead to bias with the linearly polarized measurement systems. The maximum light intensity generated by the specimen could be calculated by either using the Stokes parameters or by the least square fitting technique:

$$I = A + Sin^2(2\alpha + \omega), \tag{4.2}$$

where I is signal intensity, A is a specific constant for the microscope, α is a rotation angle and ω is a phase shift

Least square fitting results were used to calculate the parallelism index (PI) of collagen fibrils. If collagen fibrils are highly organized with the same orientation, the detected grey scale intensity reaches near zero values when the polarization plane is parallel to the collagen fibril orientation. Then, the sample fibrils behave as a single collagen fibril and the parallelism is high. In contrast, if the degree of collagen fibril organization is low, *i.e.* multiple fibril orientations are present, the minimal detected signal does not reach low values and the signal amplitude (maximum-minimal signal) is low. Multiple parameters can be derived to describe the parallelism index of collagen fibrils:
Signal ratio (S_r) can be used to measure the degree of organization as follows:

$$S_r = \frac{I_{\min}}{I_{\max}}, \tag{4.3}$$

where I_{min} is the minimal signal detected and I_{max} is the maximal signal detected, respectively.

Parallelism index (PI) (organization) of the collagen fibrils can be defined with the Michelson's contrast parameter as follows:

$$PI = \frac{I_{\max} - I_{\min}}{I_{\max} + I_{\min}}, \tag{4.4}$$

where I_{min} is the minimal signal detected and I_{max} is the maximal signal detected, respectively.

The simplest way to estimate the collagen network organization is to calculate the signal amplitude (S_{amp}) where the maximal (I_{max}) and the minimal (I_{min}) signals are subtracted and the result is used to express the degree of organization

$$S_{amp} = I_{\max} - I_{\min}, \tag{4.5}$$

Stokes parameters fully describe any polarization state of light and, therefore, all the possible polarization related information can be calculated from the Stokes parameters. Average angular information about the collagen fibrils running at the point of measurement can be derived by calculating the orientation angle of the polarization ellipse. Collagen fibril orientation and the polarization ellipse orientation angle are linked together because the collagen fibril is uniaxial. The angular information can be calculated as follows:

$$\psi = \frac{\arctan\left(\frac{S_2}{S_1}\right)}{2}, \tag{4.6}$$

where ψ=orientation angle of polarization ellipse.

4.3.3 Digital densitometry (Study I)

Spatial distribution profiles of PGs were determined using the digital densitometry of safranin-O stained cartilage sections. Cartilage tissue was prepared and 10% buffered formalin fixation was performed in the presence of safranin-O to minimize the loss of PGs during fixation. After 48 h fixation, samples were decalcified and embedded in paraffin. Histological sections (3-µm-thick) were prepared and stained with 0.5% safranin-O as described earlier (Király *et al.* 1997)**.** Safranin-O binds stoichiometrically to negatively charged GAGs of the aggrecan molecule. Therefore, it can be used for indirect estimation of PGs. Then, the PG content is directly proportional to the measured light absorption (Kiviranta *et al.* 1985).

Samples were measured with the aforementioned microscope set into the normal transmission mode equipped with an objective with magnification of x4. Sections were measured

using monochromatic light (λ=492±5μm). The system was calibrated using neutral density filters (Schott, Mainz, Germany). The linear calibration range (0-3.6 absorption units) exceeded by far the absorption measured for actual samples (max. 2 absorption units), ensuring that the measurement was not saturated. Multiple sections / sample (6 sections) were measured to reduce the effect of variable section thickness. For each measurement, a 110 pixels wide ROI was measured. Horizontal averaging was performed for each pixel row and the average value was used in the calculations. Finally, all six data vectors were averaged and the averaged result was used in the final calculations.

4.4 FOURIER TRANSFORM INFRARED IMAGING SPECTROSCOPY (STUDIES II, III AND IV)

Measurements were conducted with a Perkin Elmer Spotlight 300 imaging system (Perkin Elmer, Shelton, CO, USA), using $C0_2$-free dry air purge system (FT-IR purge gas generator, Parker Hannifin corporation, Haverhill, MA, USA).

Pure compound spectra of purified articular cartilage type II collagen and aggrecan were measured and used as reference spectra. Isolated reference material (1 mg) was mixed with KBr powder (200 mg) and homogenized. The mixture was compressed with a manual press and KBr pellets were prepared. The reference spectrum was measured using a Perkin Elmer Spotlight 300 imaging system set for point mode measurements, using 4 cm^{-1} spectral resolution, 100 μm aperture and 128 repeated scans to ensure high signal/noise-ratio.

The reference sample method was developed to reduce the effect of the variable section thickness on quantitative FT-IRIS measurements. Sections with three different nominal section thicknesses (5-, 10- and 14-μm-thick) were prepared from a single specimen of cartilage tissue (n=5 sections/each thickness). A piece of nitrocellulose western blotting membrane (Protran®, Schleicher&Schuell, Keene, NH, USA) was embedded in Tissue-

Tek® O.C.T.™ compound (Sakura Finetek, Inc., Torrance, CA, USA) and frozen together with the cartilage sample. The nitrocellulose membrane was assumed to be homogeneous in composition and, therefore, the nitrocellulose membrane absorption values were affected only by the thickness of the section. The thickness of the nitrocellulose membrane was assumed to be equal to the thickness of the cartilage sample cut at the same time. The cartilage was measured using 25μm resolution and 8 cm^{-1} spectral resolution. Two repeated scans were averaged. The thickness of the nitrocellulose membrane was ~150 μm. The edges of the membrane produced measurement artefacts due to the large refractive index differences of the membrane and the BaF_2-window material. Therefore, nitrocellulose membrane was measured using the 6.25 μm resolution. The cartilage sample was measured from articular surface to cartilage-bone junction and the average values were used for the calculations. The central part of the nitrocellulose membrane was only measured and the edges were excluded. The spectral regions for analysis of cartilage and nitrocellulose membrane were carefully selected to avoid overlapping of absorption peaks. Cartilage was measured using an average absorption of the Amide II peak (1590-1485 cm^{-1}). Nitrocellulose measurements were done using the average absorbance of 1630-1620 cm^{-1}, instead of using the whole peak to avoid saturation of the measurements. Only the offset baseline corrections were made for the samples before the measurements. The spatial distribution of collagen was estimated with the FT-IRIS (Studies III and IV). The specificity of the measurements for collagen was improved by enzymatic digestion of PGs using hyaluronidase enzyme (1000U/ml) at 37°C for 18 h (Bovine testicular hyaluronidase, type IV, H-3884, Sigma). Removal of PGs was controlled by using safranin-O staining. Only faint staining was observed after the treatments. The amount of collagen was estimated by using the average absorption of Amide I (1710-1610 cm^{-1}) (Camacho *et al.* 2002). All measurements were conducted using 8 cm^{-1} spectral and 6.25

μm spatial resolution and 2 repeated scans were averaged for each pixel.

The feasibility of utilizing qualitative cluster analysis techniques for the analysis of the properties of articular cartilage repair tissue (IV) was further investigated by applying sophisticated multivariate analysis methods. Cluster analysis provides a powerful tool for clarifying the qualitative differences in material. Analysis of the repair tissue composition is particularly well suited to multivariate analysis. Special interest was placed on the analysis of the articular cartilage collagen and on identifying the qualitative differences between intact and repair tissue. The PGs were enzymatically removed prior to the measurements. The samples were measured with Perkin Elmer Spotlight 300 imaging system using 25μm spatial resolution, 8cm^{-1} spectral resolution and 4 repeated scans per pixel. Data was pre-processed prior to the analysis by performing signal/noise-check and thickness checks. This was done to ensure removal of any foreign material and empty pixels outside the sample area. Thereafter, data was converted to the 2nd derivative spectrum and the vector normalized in order to cancel out any concentration differences. Spectral data was truncated and the spectral region of 1700-1300 cm^{-1} was selected for the final analysis. Finally, cluster analysis was carried out by using both the k-means clustering with 5-12 cluster classes and the hierarchical clustering method. In the hierarchical clustering, the distance matrix was calculated with the D-values algorithm. Ward's algorithm was chosen as the clustering method, carried out using CytoSpec software (Cytospec, CytoSpec Inc., Boston, MA, USA).

4.5 BIOCHEMICAL DETERMINATION OF COLLAGEN AND PROTEOGLYCANS (STUDY I)

Cartilage samples (Study I) were allowed to equilibrate for 2 h in phosphate buffered saline solution before determination of the wet weight. Excess water was dried with a piece of filter

paper before weighing. The samples were immersed again in buffer solution and the measurement was repeated three times. The average wet weight of the samples was used for the calculations. Thereafter the samples were lyophilized and the dry weight was measured. Lyophilization was done twice and the average weight was used. The water content of the sample was calculated using the wet and dry weights of the samples.

The amount of released PGs in the supernatant of the incubation medium containing enzyme was determined using the ethanol precipitation method. The precipitate was dissolved in water and analyzed by gel filtration of disaccharides and the uronic acid assay (Blumenkrantz & Asboe-Hansen 1973, Tammi *et al.* 2000).

The amount of hydroxyproline was used to calculate the total collagen concentration. The hydroxypyridinoline was analyzed to measure the amount of hydroxypyridinoline cross-links present in the collagen (Palokangas *et al.* 1992). The analyses were performed from three different sample pools: (1) the incubation medium, (2) the residual tissue that was first subjected to α-chymotrypsin digestion to determine the amount of denatured *vs.* intact collagen (Bank *et al.* 1997) and (3) finally the incubation medium after α-chymotrypsin digestion to investigate the amount of denatured collagen of the cartilage. Collagen samples were hydrolyzed with 6M HCl at 110ºC for 22 h. The hydrolysates were analyzed using partition chromatography (Black *et al.* 1988) and subsequently with reversed-phase high-performance liquid chromatography (HPLC) (Cheng *et al.* 1996, Eyre *et al.* 1984, Palokangas *et al.* 1992).

4.6 BIOMECHANICAL TESTING (STUDY I)

In study I, the samples were biomechanically tested using indentation geometry to determine the equilibrium Young's modulus (E_{eq}). The stepwise stress-relaxation technique with 10 repeated compression steps (1μm/s velocity, 8 min relaxation

time at each step) were applied to the maximum 20% strain. A porous cylindrical indenter (dia. = 1.0mm) was used for testing (Figure 7). A custom made computer-controlled material testing system was used for testing. The system consisted of a precision motion controller (Newport PM-500-C, Newport, Irvine, CA, USA), 1000g load cell (Sensotec, Columbus, OH, USA) and a custom-programmed data acquisition and analysis software (Labview, Austin, TX, USA) (Töyräs *et al.* 1999). The indenter force and displacement data was continuously collected during the entire measurement. Cartilage tissue was modelled as linearly elastic material and the Young's modulus was calculated as follows (Hayes etal. 1972):

$$E = \frac{P(1-\nu^2)}{2a\omega\kappa} \ , \tag{4.7}$$

where E is the Young's modulus, P is the load, υ is the Poisson's ratio (assumed to be 0.1 as previously reported (Jurvelin *et al.* 1997)), a is the indenter radius, ω is the deformation and κ is a scaling factor due to the finite and variable cartilage thickness (values are taken from previously described solutions (Hayes *et al.* 1972, Jurvelin *et al.* 1990)). In study I, Young's modulus in indentation was derived from the linear stress-strain response as follows:

$$E = E_{measured}\left(\frac{\pi a}{2h\kappa}\left(1-\upsilon^2\right)\right) \ , \tag{4.8}$$

where E is the Young's modulus, $E_{measured}$ is the modulus determined as stress/strain from experimental testing and h is the cartilage thickness.

Cartilage thickness information was acquired from a high frequency ultrasound measurement prior to the mechanical testing at the site of the indentation. After the biomechanical testing, a needle-probe technique was used to verify the cartilage thickness (Töyräs *et al.* 1999).

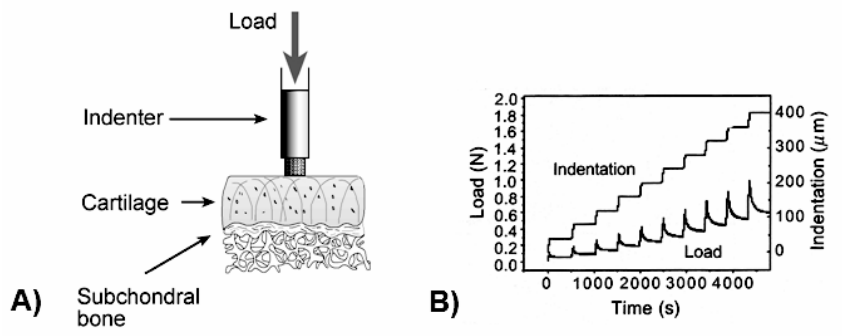

Figure 7. Schematic presentation of the indentation geometry **(A).** A porous plane-ended indenter was used to produce a local deformation (indentation) on the cartilage surface. Indentation was carried out in a stepwise manner at a constant velocity and the relaxation continued until the registered loading force became constant (equilibrium state, water movement had ceased). Multiple stress-relaxation cycles were carried out for determination of the equilibrium Young's modulus (B). A stepwise deformation of articular cartilage was produced with a precision actuator. Load and displacement were continuously monitored.

4.7 STATISTICAL ANALYSIS

Correlation coefficients between various parameters were calculated as Pearson correlation coefficients. In study I, the non-parametric Mann-Whitney U-test was used for statistical comparison of biochemical, biomechanical and microscopy parameters in different study groups. Wilcoxon signed rank test was also used for determination of the statistical difference between the cartilage thickness values obtained with the needle-probe and microscopy techniques.

In study III, the Kruskall-Wallis test was used for statistical comparison of the differences between the studied groups. Additional post hoc- contrast test for multiple analyses was carried out to determine the differences between age groups.

All statistical analysis were carried out using SPSS statistical software, versions 8.01-11.5 (SPSS inc., Chicago, IL,USA).

5 Results

5.1 ENZYMATIC DEGRADATION OF ARTICULAR CARTILAGE (STUDY I)

Enzymatic manipulation of the cartilage tissue provided new insights into the functional significance of the superficial cartilage tissue. Collagenase, chondroitinase ABC and elastase appeared to affect only the superficial tissue (I, Figure 3). No detectable changes were observed in the control groups indicating that the changes observed with enzymatic treatments were not caused by the relatively long incubation periods in use (I, Figure 4, Tables 3 and 4).

The effects of the enzymatic manipulation on the superficial cartilage with collagenase, chondroitinase ABC and elastase were undetectable with the traditional biochemical methods. The tissue showed no differences in tissue water content, amount of collagen or its cross-links when the cartilage tissue was analysed. However, the changes caused by enzymes were evident when the incubation medium was analyzed. The amount of collagen detected from the incubation medium increased by over 2000-fold after collagenase treatment, whereas neither chondroitinase ABC nor elastase had any effect on collagen (Table 3). A greater increase of the level of released hydroxylysylpyridinoline cross-links was also observed after the collagenase treatment, too. Hydroxypyridinoline cross-links were released into the incubation medium at over 14 000-fold more than from the control tissue. Hydroxylysylpyridinoline cross-links were not detected in the incubation medium after chondroitinase ABC or elastase treatments. The additional analysis of the residual tissue was performed by α-chymotrypsin treatment aiming at the estimation of denaturated collagen remaining in the tissue. The experiment showed that none of the studied groups exhibited elevated amounts of

denaturated collagen in the tissue. This indicated that chondroitinase ABC and elastase were unable to degrade collagen and that collagenase had cleaved the collagen triple-helix at several locations. The fragments released by collagenase were freely mobile and not bound to the tissue by cross-links (Table 3).

In general, the microscopic examination of the cartilage tissue was a more sensitive way of detecting local changes in the tissue than the biochemical methods. The microscopic analysis of the control groups revealed no differences, indicating that the incubation procedure itself did not cause any tissue alterations. Optical density measurements of safranin-O stained sections revealed that all three enzymes caused significant loss of PGs from the superficial cartilage tissue. Chondroitinase ABC and elastase caused more severe PG depletion than collagenase. Decreased birefringence of the superficial tissue (-65%, $p<0.01$) was observed with PLM only after collagenase treatment. The thickness of the superficial tissue also decreased by 30% suggesting that a significant amount of collagen was released from the tissue, as also verified by the biochemical analysis.

All three enzymatic treatments altered the biomechanical properties of cartilage samples. The average reduction of the Young's modulus, as compared with the controls incubated for 44h, were 45.7%, 66.2% and 44.6% for collagenase, chondroitinase ABC and elastase, respectively (Table 3). Although the collagenase enzyme degraded only collagen, it also appeared to induce secondary PG depletion by aid of diffusion of PG molecules from the degraded superficial tissue. Thus, the decreased Young's modulus probably mostly correlated with the decreased superficial tissue PG levels. The PG content of superficial tissue, measured as the optical density of the safranin-O stain, showed a statistically significant linear correlation with the equilibrium modulus ($r=0.873$, $n=71$, $p<0.001$). A high positive correlation was also acquired when the control samples were analyzed ($r=0.713$, $n=36$, $p<0.001$). The average PG content of cartilage correlated with the Young's modulus but the correlations were weaker than those obtained

from the superficial tissue (r=0.599, n=36, p<0.001 and r=0.741, n=71 (all specimens), p<0.001, respectively). The biochemical parameters appeared to be poor estimators of the tissue mechanical properties. Only the uronic acid content of the incubation medium, denoting the amount of the released PGs, had a statistically significant negative correlation with the Young's modulus ((r=-0.673, n=71, p<0.001) Table 3).

Table 3. Summary of the main biochemical, histological and biomechanical results.

	Control 0h n=24	Control 44h n=12	Collagenase n=12	Ch ABC n=10-12	Elastase n=12
Biochemical analysis of the incubation medium:					
Collagen (nmol)	-	0.31±0.16	7.16±0.81***	0.24±0.04	0.24±0.06
HP/Collagen (nmol/nmol)	-	0.11±0.05	0.60±0.10***	0.13±0.05	0.11±0.04
Uronic acid, μg	-	109.5 ±2.8	201.8 ±32.8***	584.9 ±153.5	555.0 ±177.6***
Microscopic evaluation:					
Birefringence, superficial ($x10^{-3}$)	0.34±0.07	0.28±0.10	0.17±0.05**	0.33±0.06	0.36±0.10
Optical density, superficial	1.00±0.19	0.93±0.26	0.63±0.14**	0.33±0.15**	0.56±0.20***
Optical density, average	1.74±0.16	1.67±0.27	1.60±0.19	1.35±0.17**	1.56±0.16
Biomechanical data:					
Young's modulus	1.04±0.33	1.30±0.23	0.61±0.24***	0.33±0.33***	0.65±0.36***
Peak-to-equilibrium ratio	3.72±0.76	3.70±0.73	4.26±0.80	11.14±3.59***	5.75±2.18**

Correlations with Young modulus:	**Control samples n=12-36**	**All specimens n=71**
Birefringence, superficial	-0.241 n.s.	-0.005 n.s.
Optical density, superficial	0.713***	0.873***
Optical density, full thickness	0.599***	0.741***
Collagen content	-0.140 n.s.	-0.105 n.s.
Water content	-0.211 n.s.	-0.256*
Uronic acid, incubation medium	-0.84 n.s.	-0.673***

Abbreviation: HP = hydroxylysylpyridinoline. Statistical significance was tested with Mann-Whitney U test and the levels of statistical significance were set to p<0.05 *, p<0.01 ** and p<0.001 ***. The linear correlation coefficient between the Young's modulus and related parameter is given as a Pearson correlation coefficient.

5.2 CONTROLLING THE VARIABLE CRYOSECTION THICKNESS WITH THE REFERENCE SAMPLE TECHNIQUE (STUDY II)

The quantitative use of FT-IRIS in cartilage research was evaluated in Study II. A significant section thickness variation was evident when five consecutive sections were cut and then examined with FT-IRIS. Nominal microtome cutting thickness selection was not reliable and the average infrared absorbances of five repeated measurements from 5-, 10- and 14-µm-thick sections did not linearly increase, indicating that the nominal section thickness was not accurate. For nominal cutting thickness of 5µm, 10µm and 14µm, the calculated variations of thickness (SD/mean%) were 11.5%, 12,1% and 20.6%, respectively. This error exceeds by far any acceptable error for quantitative analysis. FT-IRIS results of the individual sections displayed a considerable overlap between the groups with different section thickness.

Embedding and cutting a nitrocellulose membrane alongside with the sample provided an inexpensive and effective method to normalize the section thickness artefact. Cartilage and nitrocellulose absorbances displayed a highly linear positive correlation (r^2=0.971, n=15, p<0.001) indicating that the cartilage and reference material had been cut to the same thickness during the cryosection preparation.

FT-IRIS measurements were normalized against nitrocellulose absorption (1630-1620 cm^{-1}). The normalization reduced significantly the effect of variable section thickness. The cartilage absorption of a full thickness sample exhibited nearly constant absorbance values (0.47±0.02), independent of the cutting thickness (range 5-14 µm). The variation of measurements decreased from 14.7% (an average calculated from all sections) to 4.4%. Therefore, the reference material normalization could be used to reduce the bias caused by section thickness variation. The normalization procedure allowed the use of only a single measurement per section with a reduced risk for section thickness artefacts.

5.3 IMPROVEMENTS OF THE POLARIZED LIGHT MICROSCOPY (STUDY III)

The new instrumentation improved significantly the capability of the PLM to produce new information on the cartilage tissue. The enhanced polarized light microscope system allowed more precise characterization of the collagen network properties both in qualitative and quantitative terms. The earlier instrument allowed only the quantitative measurement of birefringence and qualitative visualization of articular cartilage. The new system made it possible to determine the Stokes parameters for complete characterization of the polarization phenomenon. The main differences between the previously used and updated PLM systems are summarized in Table 4.

Table 4: Summary of the modifications made to the previously used polarized light microscope and a list of the benefits acquired with the modifications.

Instrument modications:	Acquired improvements:
Lamphouse thermostabilization and improved power supply	**Stable illumination for longer periods** -Reproducibility of birefringence measurements -Longer lamp-life **Brighter illumination** -Shorter exposure time
Precision grade optics -Polarizers -Phase shifter	**Increased polarization purity** -Decreased background levels
Additional monochromator -591±10nm -594±3nm (new)	**Near laser-grade monochromacy (±3nm)** -Fulfils better the theoretical monochromacy demand
Computer-controlled rotation tables -0.01° resolution for angular rotation	**Automated system** -Alignment, calibration and measurement
Changed measurement principle -Use of multiple images	**Determination of the Stokes parameters** -Orientation independent birefringence -Collagen fibril orientation -Collagen fibril parallelism

The parallelism index was introduced as a new parameter which would describe the degree of organization of the collagen fibrils (III). The parallelism index describes the degree of parallelism with which the collagen fibril bundles are aligned within a pixel. The parallelism index represents a new

parameter to follow and register the organization of the collagen fibrils (III). The parallelism index was not affected by the collagen fibril orientation and it was less affected by the amount of collagen content than the previously used birefringence parameter. Collagen fibril orientation could be calculated using either the Stokes parameters or the least-square fitting method (III and IV). Orientation describes the average orientation of the collagen fibrils within the pixel area in relation to the cartilage surface. The least square fitting method offered a straightforward solution for calculating the orientation without any specialized software. The average fibril orientation was calculated from the phase-shift of the fitting result. This approach was favourable when the signal-to-noise ratio was low on account of the fact that the measurements were now more insensitive to random noise than from the individual single images. The signal-to-noise ratio was substantially lower in the low birefringent regions of the sample (intermediate zone). Random noise may jeopardize the accuracy of the measurement results if the information is collected only from a single image. The least square fitting was carried out using seven separate images and the actual values were taken from the fitting result. Therefore, the net effect of noise was minimized and accuracy of the measurement was maintained even with the low signal areas of the sample. The control of the polarizers and image capturing were computer-controlled. The new PLM system was designed to minimize the possibility of user-derived systematic errors. To achieve this aim, each time that the system was turned on, the alignment and calibration of the system were performed automatically. The microscope can be calibrated for weak (cartilage) or strong (bone) birefringence. Dual exposure times can also be used (cartilage sample with subchondral bone) with ideal calibration results (R^2=1.000).

The stability of the new PLM system was tested by repeated measurements of the same sample. The experiment was carried out to test whether the illumination of the system was stable when lamphouse cooling and stability of the electric supply control were improved. The new PLM system proved to be very

stable. Only a 0.8% increase of the detected signal was noticed over a 5h period indicating that calibration was stable for a long period. The reproducibility of the measurement system was tested. All of the parameters showed similar results when the same sample was measured for 10 repeated times. The coefficient of variation (rms CV) was tested for full thickness cartilage in 10% fractions from superficial to deep cartilage. The detected variation was 0.79% for birefringence, 0.23% for orientation and 0.40% for parallelism (III). The results indicated that the measurement technique gave highly reproducible data and the bias caused by the PLM system was very low.

It has been previously suggested that birefringence is also an estimator of collagen content (Arokoski *et al.* 1996). The present findings, however, indicated that birefringence was not directly related to the collagen content (III and IV) but instead it was also related to collagen fibril organization. The linear correlation between the FTIR-derived collagen content and the birefringence varied from being excellent to non-existent (or even to a negative correlation) depending on the maturation stage of the sample (Figure 8). The highest correlations between the birefringence and the collagen content were present in fully mature tissue. At that time the collagen network had stabilized and the collagen fibril organization reached its highest values (IV, n=12, mean R^2=0.82±0.12, $p<0.001$). Eleven-month-old porcine samples showed the lowest association between the collagen content and the birefringence (IV, n=12, R^2=0.22±0.28, n.s.). The results between the collagen content and birefringence were a clear indication that birefringence cannot be used as an estimator of the collagen content. In other words, birefringence is significantly influenced by collagen organization.

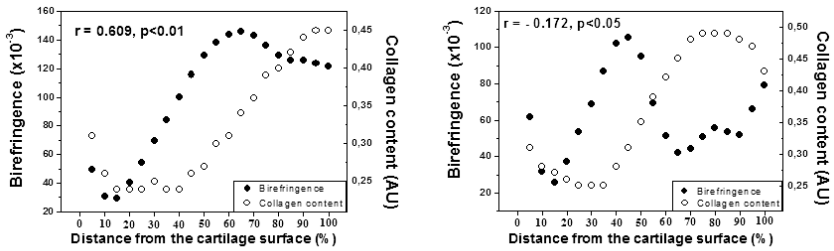

Figure 8. Comparison of polarized light microscopy derived birefringence and FTIR derived collagen content from fully mature (A) and juvenile (B) bovine tissue. The correlation between birefringence and collagen content is not the same for all tissue types. Several factors, such as collagen fibril diameter, degree of organization, packing of the individual fibrils, affect the measured birefringence values. The linear correlation between the birefringence and collagen content can vary from highly positive to negative correlation depending on the tissue type.

5.4 FUNCTIONAL ADAPTATION OF THE COLLAGEN NETWORK PROPERTIES DURING TISSUE MATURATION (STUDY IV)

The development and functional adaptation of collagen network of porcine articular cartilage were monitored with polarized light microscopy and FT-IRIS. The main findings given as average values for the full cartilage thickness are summarizd in Table 4.

Changes of the porcine articular cartilage were investigated at 4 months, 11 months and 21 months of age. The collagen network underwent substantial remodelling during growth and maturation. The cartilage phenotype of young animals was different from the phenotype of mature bovine and adult human cartilage, as earlier described by Benninghoff (Benninghoff 1925) (Figure 10 and Table 5). At 4 months of age, the collagen fibrils were highly organized and, throughout the tissue depth, the preferential collagen fibril orientation was parallel with the surface (IV, Figures 2 and 4). The structure of the collagen network at 11 months of age reflected the rearrangement of the collagen network as the degree of

horizontal organization decreased and the preferential course of collagen fibrils started to resemble that present in the adult tissue (IV, Figure 4). The parallelism index reached its lowest values in the 11 month-old-animals, possibly as an indication of the re-organization of the collagen network as tissue maturation progressed. By 21 months of age, the collagen network had already become highly organized and arranged as described by Benninghoff (1925) (IV, Figures 2 and 4). The superficial cartilage tissue had tightly packed collagen fibrils arranged parallel to the surface. After arching of the fibrils into the intermediate zone, the deep tissue showed highly organized collagen fibrils running perpendicular to the cartilage surface. Fully mature porcine cartilage had a similar visual appearance as the fully mature human tissue, indicating that the mature phenotype of the articular cartilage is similar in both species (Figure 9).

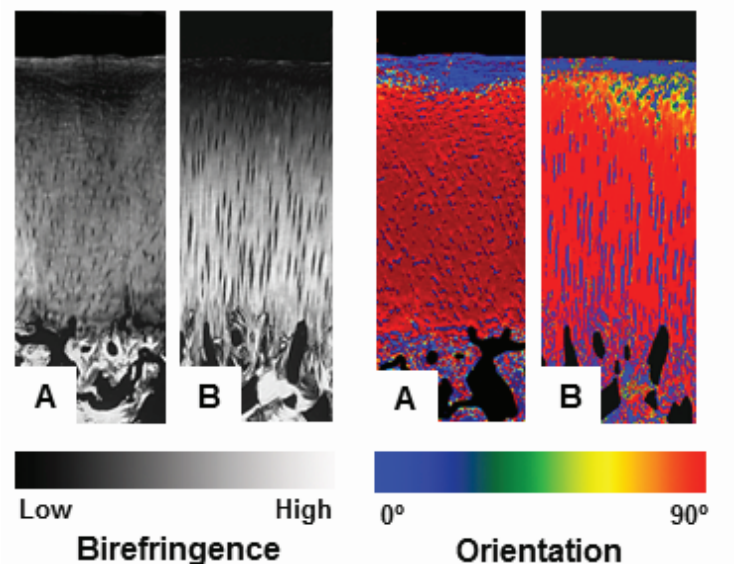

Figure 9. Comparison of the collagen network architecture of adult human cartilage (A) and 21-month-old porcine (mature tissue) cartilage (B). Both species show an identical collagen network configuration when the final phenotype is achieved. Immature porcine cartilage displayed a completely different collagen network architecture.

The amount of collagen (estimated by FT-IRIS Amide I absorption) significantly increased during growth and development. The average absorptions were 0.18±0.04, 0.26±0.04 and 0.32±0.07 at 4, 11, and 21 months of age, respectively (Table 5). The spatial distribution of collagen differed even more than the average content. The deep cartilage tissue exhibited an over 4-fold increase in the amount of collagen content (IV, Figure 4a). The FT-IRIS studies allowed also the analysis of maturation changes which occur in the territorial and interterritorial matrices. The interterritorial matrix revealed a condensation of collagen fibrils whereas the territorial matrix possessed a high amount of PGs but had relatively low collagen levels (IV, Figure 7).

Table 5. Changes of collagen network of articular cartilage during porcine maturation. The values are given as averages for the whole thickness.

Age	Cartilage thickness (µm)	Collagen content (Abs.)	Collagen Orientation (degrees)	Collagen parallelism index	Birefringence (10^{-3})
4 months	2294±569	0.18±0.04	27.3±8.6	72.4±13.6	0.49±0.12
11 months	1141±238**	0.27±0.04**	47.8±21.4	53.7±5.3**	0.50±0.13
	-50%	+150%	+175%	-26%	+2%
21 months	790±117***	0.33±0.06***	75.9±5.5***	70.8±3.4	1.48±0.55***
	-66%	+183%	+278%	-2%	+302%

Absolute values ± standard deviations are given and the changes in percentage in comparison to the 4-month-old group. Statistical differences were tested using the non-parametric Kruskall-Wallis test. Statistical significance was compared with the 4-month-old samples. **$p<0.01$ and ***$p<0.001$.

5.5 NEW UNPUBLISHED RESULTS

5.5.1 Polarized light microscopy

In linear PLM, the presence of non-birefringent cell lacunae did not caused any significant analysis error when the whole tissue was included in the measurements. In the new PLM technique, orientation and parallelism index of collagen network were calculated individually for all pixels of the image area, also including the cell lacunae. This was a potential source of error since the cell lacunae are empty holes, *i.e.* non-birefringent areas. The proportion of the possible error was tested using a tissue with high cellularity (4-month-old porcine cartilage) and fully mature tissue with low cell density (21-month-old porcine cartilage) (Figure 10). The cell areas were manually excluded from the analysis. The effect of the biased values was compared either to untreated or to median filtered images (5x5 median filter).

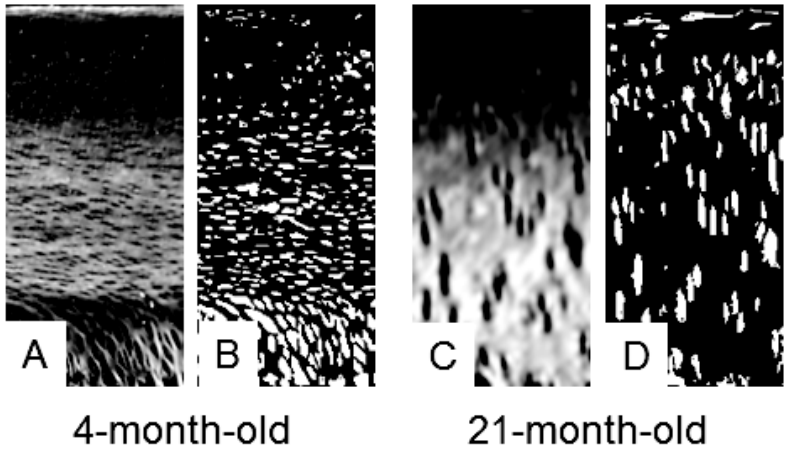

Figure 10. The non-ECM areas that were included in the measurements (cell lacunae) of 4-month-old (A) and 21-month-old (C) porcine cartilages. The binary segmental images (B and D) indicate the area of cell lacunae (white) that needs to be excluded from the analysis.

The results indicated that the parallelism index was affected by inclusion of the cell lacunae in the calculations. Removal of

the cell lacunae changed the measurement results by 6.2±5.9% for the high cell density samples and 2.3±2.1% for the low cell density samples, as compared with the values of untreated tissue. Application of median filtering with 5x5 pixel filter reduced the cell effect to 3.7±5.7% and 0.1±0.2%, respectively. The median filtering was less effective in those areas where there were sharp changes in the parallelism index, such as the intermediate zone.

A similar effect was detected when the changes in the collagen fibril orientation were tested. The cell effect was -12.6±19.1% for 4-month-old samples and 3.5±9.1% for 21-month-old samples. The median filtering reduced the bias to 2.0±14.7% and 2.1±9.3% for samples from 4-month-old and 21-month-old animals, respectively.

5.5.2 Fourier transform infrared imaging

Fourier transform infrared imaging offered a tool to characterize cartilage tissue composition as chemical maps, preserving at the same time the spatial information. It was obvious that the applicability of the FT-IRIS technique was still hindered by the incomplete molecular specificity of the current data-analysis techniques. The results indicated that the Amide I absorption peak (wavenumbers 1710-1610 cm^{-1}) could not be regarded as being specific for the estimation of collagen content. Amide I absorption decreased by 25.3% when the sections were investigated after hyaluronidase enzyme treatment which removes the PGs. The observed systematic decrease was evident with all tested samples and the difference achieved a high statistical significance ($p<0.01$) (Figure 11).

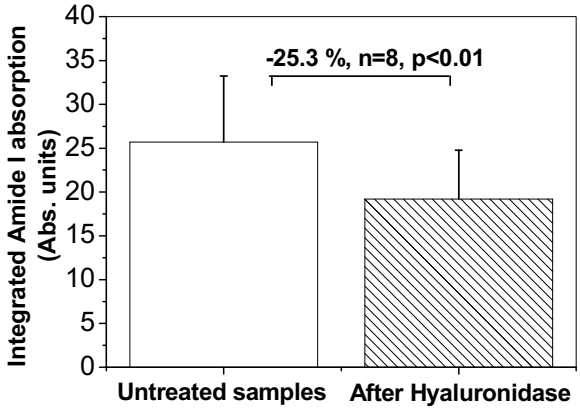

Figure 11. Amide I absorption (1710-1610 cm^{-1}) has been previously used for estimation of the collagen content. Bovine articular cartilage specimens (N=8) were measured before and after hyaluronidase treatment, *i.e.* removal of the PGs. A systematic, statistically significant reduction of the Amide I absorption was observed indicating that PGs can influence the Amide I parameter. Therefore, Amide I absorption cannot be regarded as a reliable estimator of pure collagen content.

The application of modern cluster analysis enabled a detailed qualitative analysis of articular cartilage composition. Mathematical analysis of spectral differences was utilized to analyse compositional changes without any *a priori* knowledge of the possible different spectroscopic features. This method was briefly tested in order to investigate whether articular cartilage repair tissue differs from the adjacent native tissue. The clustering approach was tested using the second derivative spectra. The data was vector-normalized to cancel out any concentration changes. Both the k-means clustering and the hierarchical cluster analysis identified a difference between the repair and the native tissue, suggesting that there were differences in the chemical composition of those tissues. The k-means cluster image closely agreed with the reference type II collagen immunohistochemistry (Figure 12). Analysis of the spectral data obtained from the intact and repair cartilage revealed several differences throughout the analysis area (Figure 13).

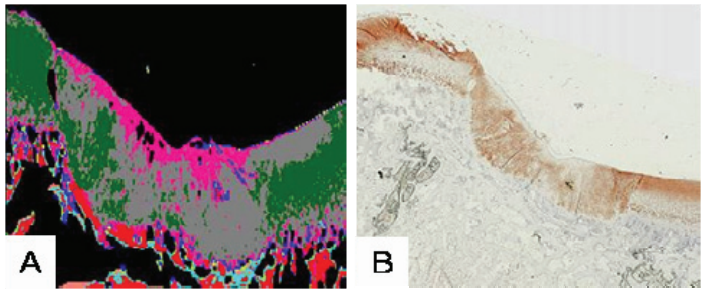

Figure 12. Pictures of the FT-IRIS k-means clustering map (second derivative spectral analysis) (A) and a histological cartilage section stained with type II collagen antibody (B) that reveals a cartilage defect and surrounding intact cartilage. Clustering of the FT-IRIS map is done by mathematical calculation without any user intervention or any *a priori* information about the tissue properties. Grey colour represents repair tissue, pink most likely is tissue originating from the periosteal flap and the green colour indicates the surrounding intact cartilage.

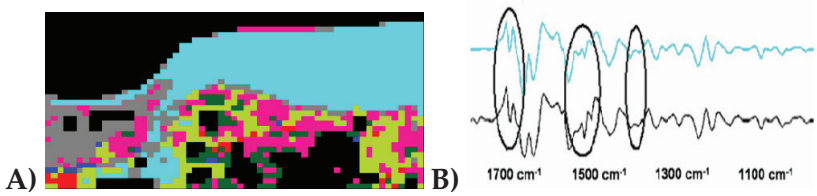

Figure 13. FT-IRIS cluster map from a cartilage repair sample (A). The cluster analysis was performed using the second derivative spectra and hierarchical cluster analysis. Hyaluronidase treatment was used to remove PGs from the cartilage sample. Therefore, the detected clustering was most likely due to the differences related to the collagen network. During pre-processing, the data were vector-normalized in order to cancel out any absorption differences. Blue colour represents the intact cartilage area and the grey area is repair tissue. Comparison between the 2nd derivative spectrum of the native cartilage (light blue) and the repair tissue (grey) is shown (B). The repair tissue displays the largest differences at 1700 cm^{-1}, 1500cm^{-1} and 1390cm^{-1}.

5.5.3 Cartilage maturation

Changes observed during maturation of porcine tissue were compared with alterations of human tissue during growth. The human tissue seemed to undergo similar cartilage remodelling as seen in the porcine tissue, suggesting that these changes may be common in all mammals. The postnatal human tissue showed only faint birefringence as compared to the mature human cartilage (unpublished data). This was most likely due to a low amount of collagen and the low degree of organization of collagen fibrils. Furthermore, a cartilage specimen taken from a 7-year-old child showed similar collagen network structure to that of the 11-month-old porcine cartilage, *i.e.* the collagen fibrils were still arranged predominantly in a parallel direction to the surface, also in the deep tissue (Figure 14). Both species showed identical collagen network arrangement when the maturation period had ended (Figures 9 and 14).

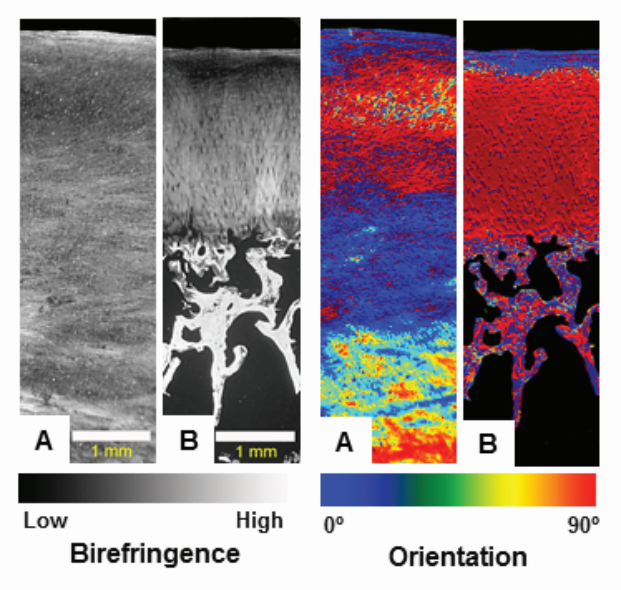

Figure 14. Immature human cartilage from a 7-year-old child (A) shows multilaminar collagen structure. Adult human cartilage (B) has the typical tri-laminar structure described by Benninghoff (1925).

6 Discussion

6.1 CHARACTERIZATION OF ARTICULAR CARTILAGE PROPERTIES WITH POLARIZED LIGHT MICROSCOPY AND DIGITAL DENSITOMETRY

The development of the PLM has greatly increased the applicability of the technique for cartilage research. PLM is one of the few techniques that can be used for visualization of the collagen network architecture. The technique allows visualization of the entire section from cartilage surface to the cartilage-bone interface within one single image. In study III, there was a special emphasis on developing further the existing polarized light microscopy instrumentation and methodology. PLM has been used for decades for the characterization of the collagen network properties.

First, the light microscope using linearly polarized light was utilized to determine qualitative and quantitative properties (*i.e.* birefringence) of the collagen fibrils. Birefringence was the only measurable quantitative parameter. Linearly polarized light measurements were affected by the variable detection sensitivity for the true birefringence generated by the sample. The detected signal intensity was dependent on the collagen fibril orientation (and the orientation of the sample between crossed polarizers).

Quantitative microscopy proved to be a sensitive technique to observe local and small compositional changes generated by enzymatic manipulation (I). Digital densitometry of safranin-O stained cartilage showed a high correlation with the biomechanical properties (I). The superficial zone PG content showed the highest correlation and, therefore, appeared to highlight the importance of the structure and function of the superficial tissue of articular cartilage (I). Digital densitometry measurements could give biased results on account of the

variable section thickness. No microtome can produce sections with constant thickness, especially when only 3-µm-thick sections need to be cut. The variable section thickness prevents any comparison of different specimens when only single measurements are made. In practice, however, the laboratory costs and time required for producing multiple sections was not a limiting factor for the use of the technique. The routine measurements were quick to perform when multiple sections were examined. Digital densitometry of cationic safranin-O stain, or some other cationic stain used for PG quantification, has proved to be an invaluable reference technique in studies where there is a special interest on the characterization of local PG distribution. The method has been used successfully in conjunction with MRI, ultrasound and Fourier transform infrared imaging studies (Nieminen *et al.* 2002, Nieminen *et al.* 2002, Nissi *et al.* 2004, Rieppo *et al.* 2010a).

Study III was carried out to update PLM instrumentation, software and methodological aspects of the technique. Topo-optical enhancer stains were no longer needed to enhance the birefringence, since the modern CCD-camera technology permitted detection of weak signals from cartilage tissue. Thus, transparent cartilage samples can be recommended for quantitative work. Thus, the uncertainty concerning the binding of the topo-optical dyes and the signal enhancement can be avoided. The instrumentation designed and used in study III, made it possible to determine the Stokes parameters. In principle, the Stokes parameters describe completely the polarization phenomenon and, therefore, the whole possible polarization-related information can be calculated from the measured data.

The new improved PLM system allowed more precise qualitative and quantitative characterization of the collagen network properties (III and IV). The collagen fibril orientation could be calculated (III and IV) to describe the average orientation of the collagen fibrils within the pixel area in relation to the cartilage surface. The least square fitting offered a straightforward solution for calculating the orientation without

any specialized software. The parallelism index was introduced as a new parameter which would describe the degree of organization of the collagen fibrils, *i.e.* how parallel the fibril bundles are aligned within a pixel (III). Thereby, the parallelism index represented a parameter to follow and register the organization of the collagen fibrils alone (III). It was not affected by the collagen fibril orientation and was less affected by the amount of collagen than the previously used birefringence parameter.

Our results indicate that one can obtain repeatable measurements of birefringence, collagen fibril orientation and parallelism with the PLM device. The error due to the microscope itself is negligible as compared to the possible errors introduced during sample preparation. Multiple sections and preferably multiple cutting directions should be used to cancel out any variations in the section thickness and this will also eliminate the possible effect of preferential collagen fibril orientation in the superficial tissue.

Data analysis seems to be the most crucial source for errors in PLM studies. The present results indicate that the effect of cell lacunae has to be considered when PLM derived collagen PI and fibril orientation are determined. Errors induced by the cells exceed by far the measurement error caused by the technique itself and they cannot be simply neglected when the cell densities vary, e.g. during tissue maturation. Median filtering of the images offers a satisfactory and simple tool for reducing the cell lacunae bias without resorting to laborious manual image segmentations. However, the spatial pixel resolution has to be reduced in order to have the median filter to be efficient. The size of the cell lacunae exceeds the typical spatial resolution of polarized light microscopy and therefore even a 5x5 median filter may not reduce the cell effect properly. It was found that the median filter works more effectively when the pixel size is similar to the size of the individual cell lacunae.

The biomechanical properties of articular cartilage cannot be understood if the tissue is modelled simply as a homogenous mixture of water, collagen and PGs. The collagen network

architecture has a highly specialized functional significance. Sophisticated cartilage modelling has incorporated properties of the collagen network structure into the mathematical models and, therefore, one can obtain realistic theoretical calculations of the tissue properties (Julkunen *et al.* 2007). In the present study, PLM proved to be an excellent tool for achieving a detailed quantitative characterization of the collagen network properties (IV). Recent progress in the field of PLM might even permit visualization of the three-dimensional collagen structure (Oldenbourg 2008). The information generated with polarized light microscopy cannot be obtained from biochemical techniques.

6.2 APPLICATION OF FOURIER TRANSFORM INFRARED IMAGING SPECTROSCOPY IN CARTILAGE RESEARCH

Fourier transform infrared imaging spectroscopy is a relatively new technique in cartilage research. FT-IRIS holds the potential to become an important tool for characterization of the spatial distribution of articular cartilage constituents. One unique feature of FT-IRIS is that it can be used for the simultaneous determination of collagen and PG contents. Theoretically, infrared absorption produces a "chemical fingerprint" of the tissue constituents, *i.e.* information about the spatial chemical composition. In FT-IRIS, individual pure compound information about collagen, aggrecan, *etc.,* is superimposed and the sum of the infrared absorption derived from all tissue components is measured. Therefore, it is essential to develop sensitive parameters for specific tissue constituents. FT-IRIS absorption is directly proportional to the section thickness, analogously with digital densitometry and PLM. FT-IRIS measurements can take a long time depending on the choice of measurement routines, *i.e.* spatial and spectral resolution and the amount of repeated scans. Variable section thickness is a particular problem when frozen sections are being used. The reference method (II) can significantly reduce the measurement bias. Frozen sections offer

a minimally altered tissue composition as no chemical fixation is needed. Unfortunately, frozen sections from cartilage tissue cannot be cut with accurate control of the section thickness, as demonstrated in study II. Optimization of the measurement time is necessary if one wishes to conduct larger studies, *e.g.*, with more than 50 samples. Depending on the selected measurement parameters and measured area, the measurements may take hours to perform. For these practical reasons, in order to optimize the measurement time without compromising the data quality, the reference sample technique can reduce the amount of work by 80% without interfering with the repeatability of the measurements (II).

The recently published FT-IRIS study questioned the specificity of the previously used parameters for PG measurement (Rieppo *et al.* 2010a). It was demonstrated that the specificity of the PG parameter could be improved when more advanced analysis tools were used (Rieppo *et al.* 2010a). In this thesis, the specificity of the previously used collagen parameter (Amide I) was also found to be inadequate to allow a specific quantification of collagen. With the systematic development of parameters for quantitative analysis of collagen and PG contents, FT-IRIS may represent a specific tool capable of characterizing the tissue properties from histological sections. Ongoing research projects suggest that FT-IRIS can reach at least the specificity level of safranin-O staining, and a similar type of application may well also be developed for collagen analysis (Närhi *et al.* 2010, Rieppo *et al.* 2010a, Rieppo *et al.* 2010b). Currently, collagen analysis with FT-IRIS requires enzymatic removal of PGs, as was done in studies III and IV. Even with the present parameters, FT-IRIS has proven its potential for use in cartilage research. Polarization aspects have been brought up also for FT-IRIS studies. Collagen fibril orientation as well as the specific changes in molecular level can be studied with FT-IRIS (Bi *et al.* 2005, Ramakrishnan *et al.* 2007, Xia *et al.* 2008, Xia *et al.* 2007). FT-IRIS results have also been implemented in finite element studies investigating the biomechanical properties of

articular cartilage (Julkunen *et al.* 2008, Korhonen *et al.* 2006, Saarakkala *et al.* 2009).

Our pilot studies suggest that sophisticated multivariate cluster analysis techniques can be used for characterization of the qualitative differences in material properties of articular cartilage (Rieppo *et al.* 2007). In cluster analysis, the extent of absorption is normalized (concentration changes are eliminated) and the analysis is performed to determine whether any spectroscopic differences can be observed. This approach has advantages, *e.g.* when tissue maturation or articular cartilage repair experiments are analysed. The data are mathematically arranged in clusters with similar spectroscopic features. For example, the repair tissue seems to form a separate cluster in comparison with the adjacent native tissue, enabling identification of the repair tissue by its infrared absorption properties. If the repair tissue shows maturation and is able to form normal-looking cartilage, it should be possible to detect differences in clustering of the tissue. Optimally, the repair tissue cluster should disappear. Furthermore, qualitative cluster analysis can be combined with quantitative compositional analysis and then both the amount and the type of tissue can be analysed at the same time. The spectroscopic approach could open a new era for FT-IRIS-related cartilage studies.

6.3 MATURATION-RELATED CHANGES AND PROPERTIES OF ARTICULAR CARTILAGE COLLAGEN NETWORK

In Study IV, the changes of collagen network were characterized during postnatal growth and maturation of the cartilage tissue. It is known that the biochemical composition of cartilage changes during maturation. However, the simultaneous architectural changes in collagen network have remained unclear. The present study revealed that the cartilage tissue present in a young subject will change drastically during maturation. At a young age, the predominant collagen fibril orientation is parallel to the cartilage surface throughout the

tissue depth. Over time it gradually achieves the tri-laminar appearance originally described by Benninghoff (Benninghoff 1925). The collagen fibril organization of young individuals is lost during growth and a new type of network is created as the collagen is laid down (IV). Most likely the original collagen network present at birth is poorly organized, and subsequently it starts to be re-arranged. Increased body weight and joint loading most likely evoke the reorganization, and the tissue becomes remodelled to adapt to the biomechanical demands imposed by normal locomotion. It is known that the same process takes place in equine (Brama *et al.* 2009, Hyttinen *et al.* 2009) and human cartilage. Recent MRI studies have shown that the number of laminar structures of cartilage, detected with T_2-measurements, decrease with age (Hannila *et al.* 2009). This finding is well in good agreement with the present findings regarding the normal tissue maturation process.

These present findings indicate that cartilage maturation takes a long time (IV). The final cartilage phenotype is reached at an age that possibly corresponds to 12-18 years of human life. This lengthy process should be taken into account when cartilage studies are conducted with animal models. Bovine and porcine tissues are most often obtained from abattoirs. The typical lifespan for animals bred for meat production is four months for pigs and between 11 and 18 months for bovines. Porcine tissue has not reached the mature structure at that early age (IV). In addition the bovine cartilage may take longer maturation period, as suggested by multiple laminar structures and the variation of the number of laminae detected in Study I (Nieminen *et al.* 2000). The increased variability of the biomechanical behaviour of cartilage tissue may also be related to variations in the stage of tissue maturation, *i.e.* the sample material might include animals at different stages of maturation. This needs to be taken into account when the maturation-related biomechanical experiments are conducted or when the results from different experiments are compared.

7 Conclusions

Quantitative imaging techniques represent a way to achieve a detailed characterization of the articular cartilage composition. Microscopic imaging techniques are complementary to the biochemical techniques though they provide spatial information which is impossible to obtain with conventional biochemical tools. Fourier transform infrared imaging spectroscopy holds extensive potential for becoming an important method for biochemical characterization of articular cartilage. However, the effective use of spectroscopy will require the further development of sophisticated data analysis methods.

The main results of this study can be summarized as follows:

- Quantitative microscopy can detect sensitively spatial changes in the composition and architecture of cartilage tissue (Study I).
- Applicability of polarized light microscopy for cartilage research is significantly improved with novel microscope instrumentation and with the application of the Stokes parameters (Study III).
- Fourier transform infrared imaging can be used for simultaneous imaging of the spatial distribution of collagen and PG contents in articular cartilage. Furthermore, the cluster analysis method can be used to study qualitative material properties of articular cartilage (Studies II and IV and additional data presented in this thesis)
- Superficial PG content controls significantly the equilibrium stiffness of bovine articular cartilage in indentation geometry (Study I).
- The collagen network undergoes significant remodelling during growth and maturation of porcine articular cartilage. Tissue maturation proved to be slow and this is a factor that has to be taken into account when studies are carried out with experimental animals. The observed tissue changes support the concept that cartilage properties can be affected by physical exercise at a young age (Study IV).

References

1. Adany, R., Modis, L., and Balogh, G. (1979) A critical re-evaluation of the anisotropic index used in polarization microscopy: a study on epiphyseal cartilage, *Acta Histochem 65*, 243-249.
2. Alhadlaq, H. A., and Xia, Y. (2004) The structural adaptations in compressed articular cartilage by microscopic MRI (microMRI) T(2) anisotropy, *Osteoarthritis Cartilage 12*, 887-894.
3. Altman, R. D. (2010) Early management of osteoarthritis, *Am J Manag Care 16 Suppl Management*, S41-47.
4. Arokoski, J., Jurvelin, J., Kiviranta, I., Tammi, M., and Helminen, H. J. (1994) Softening of the lateral condyle articular cartilage in the canine knee joint after long distance (up to 40 km/day) running training lasting one year, *Int J Sports Med 15*, 254-260.
5. Arokoski, J., Kiviranta, I., Jurvelin, J., Tammi, M., and Helminen, H. J. (1993) Long-distance running causes site-dependent decrease of cartilage glycosaminoglycan content in the knee joints of beagle dogs, *Arthritis Rheum 36*, 1451-1459.
6. Arokoski, J., Malmivaara, A., Manninen, M., Moilanen, E., Ojala, R., Paavolainen, P., Ruuskanen, J., Virolainen, P., Virtapohja, H., Vuolteenaho, K., and Österman, H. (2007) Polvi- ja lonkka nivelrikon hoito, *Duodecim 123*, 602-620.
7. Arokoski, J. P., Hyttinen, M. M., Lapveteläinen, T., Takacs, P., Kosztaczky, B., Modis, L., Kovanen, V., and Helminen, H. (1996) Decreased birefringence of the superficial zone collagen network in the canine knee (stifle) articular cartilage after long distance running training, detected by quantitative polarised light microscopy, *Ann Rheum Dis 55*, 253-264.
8. Bae, W. C., Wong, V. W., Hwang, J., Antonacci, J. M., Nugent-Derfus, G. E., Blewis, M. E., Temple-Wong, M. M., and Sah, R. L. (2008) Wear-lines and split-lines of human patellar cartilage: relation to tensile biomechanical properties, *Osteoarthritis Cartilage 16*, 841-845.

9. Bank, R. A., Bayliss, M. T., Lafeber, F. P., Maroudas, A., and Tekoppele, J. M. (1998) Ageing and zonal variation in post-translational modification of collagen in normal human articular cartilage. The age-related increase in non-enzymatic glycation affects biomechanical properties of cartilage, *Biochem J 330*, 345-351.
10. Bank, R. A., Krikken, M., Beekman, B., Stoop, R., Maroudas, A., Lafeber, F. P., and te Koppele, J. M. (1997) A simplified measurement of degraded collagen in tissues: application in healthy, fibrillated and osteoarthritic cartilage, *Matrix Biol 16*, 233-243.
11. Bank, R. A., Soudry, M., Maroudas, A., Mizrahi, J., and TeKoppele, J. M. (2000) The increased swelling and instantaneous deformation of osteoarthritic cartilage is highly correlated with collagen degradation, *Arthritis Rheum 43*, 2202-2210.
12. Bayliss, M. T., and Ali, S. Y. (1978) Age-related changes in the composition and structure of human articular- cartilage proteoglycans, *Biochem J 176*, 683-693.
13. Belbachir, K., Noreen, R., Gouspillou, G., and Petibois, C. (2009) Collagen types analysis and differentiation by FTIR spectroscopy, *Anal Bioanal Chem 395*, 829-837.
14. Bennett, H. S. (1950) Methods applicable to the study of both fresh and fixed materials. The microscopical investigation of biological materials with polarized light, in *McClung's handbook of microscopical technique* (McClung, J. R., Ed.), pp 591-677, Paul B Hoeber, New York.
15. Benninghoff, A. (1925) Form und Bau der Gelenkknorpel in ihren Beziehungen zur Function. Erste Mitteilung: die modellierenden und formerhaltenden Faktoren des Knorpelreliefs., *Z Anat 76*, 43-63.
16. Berenbaum, F. (2008) New horizons and perspectives in the treatment of osteoarthritis, *Arthritis Res Ther 10 Suppl 2*, S1.
17. Bi, X., Li, G., Doty, S. B., and Camacho, N. P. (2005) A novel method for determination of collagen orientation in cartilage by Fourier transform infrared imaging spectroscopy (FT-IRIS), *Osteoarthritis Cartilage 13*, 1050-1058.

18. Bi, X., Yang, X., Bostrom, M. P., Bartusik, D., Ramaswamy, S., Fishbein, K. W., Spencer, R. G., and Camacho, N. P. (2007) Fourier transform infrared imaging and MR microscopy studies detect compositional and structural changes in cartilage in a rabbit model of osteoarthritis, *Anal Bioanal Chem 387*, 1601-1612.
19. Bi, X., Yang, X., Bostrom, M. P., and Camacho, N. P. (2006) Fourier transform infrared imaging spectroscopy investigations in the pathogenesis and repair of cartilage, *Biochim Biophys Acta 1758*, 934-941.
20. Bjelle, A. (1975) Content and composition of glycosaminoglycans in human knee joint cartilage. Variation with site and age in adults, *Connect Tissue Res 3*, 141-147.
21. Black, D., Duncan, A., and Robins, S. P. (1988) Quantitative analysis of the pyridinium crosslinks of collagen in urine using ion-paired reversed-phase high-performance liquid chromatography, *Anal Biochem 169*, 197-203.
22. Blumenkrantz, N., and Asboe-Hansen, G. (1973) New method for quantitative determination of uronic acids, *Anal Biochem 54*, 484-489.
23. Bolton, M. C., Dudhia, J., and Bayliss, M. T. (1999) Age-related changes in the synthesis of link protein and aggrecan in human articular cartilage: implications for aggregate stability, *Biochem J 337 (Pt 1)*, 77-82.
24. Brama, P. A., Bank, R. A., Tekoppele, J. M., and Van Weeren, P. R. (2001) Training affects the collagen framework of subchondral bone in foals, *Vet J 162*, 24-32.
25. Brama, P. A., Holopainen, J., van Weeren, P. R., Firth, E. C., Helminen, H. J., and Hyttinen, M. M. (2009) Influence of exercise and joint topography on depth-related spatial distribution of proteoglycan and collagen content in immature equine articular cartilage, *Equine Vet J 41*, 557-563.
26. Brama, P. A., Tekoppele, J. M., Bank, R. A., Barneveld, A., Firth, E. C., and van Weeren, P. R. (2000) The influence of strenuous exercise on collagen characteristics of articular cartilage in Thoroughbreds age 2 years, *Equine Vet J 32*, 551-554.

27. Brama, P. A., TeKoppele, J. M., Bank, R. A., Barneveld, A., and van Weeren, P. R. (2002) Development of biochemical heterogeneity of articular cartilage: influences of age and exercise, *Equine Vet J 34*, 265-269.
28. Brama, P. A., Tekoppele, J. M., Bank, R. A., Barneveld, A., and van Weeren, P. R. (2000) Functional adaptation of equine articular cartilage: the formation of regional biochemical characteristics up to age one year, *Equine Vet J 32*, 217-221.
29. Brama, P. A., Tekoppele, J. M., Bank, R. A., Karssenberg, D., Barneveld, A., and van Weeren, P. R. (2000) Topographical mapping of biochemical properties of articular cartilage in the equine fetlock joint, *Equine Vet J 32*, 19-26.
30. Brama, P. A., TeKoppele, J. M., Beekman, B., van El, B., Barneveld, A., and van Weeren, P. R. (2000) Influence of development and joint pathology on stromelysin enzyme activity in equine synovial fluid, *Ann Rheum Dis 59*, 155-157.
31. Brama, P. A., TeKoppele, J. M., Beekman, B., van Weeren, P. R., and Barneveld, A. (1998) Matrix metalloproteinase activity in equine synovial fluid: influence of age, osteoarthritis, and osteochondrosis, *Ann Rheum Dis 57*, 697-699.
32. Brama, P. A., van den Boom, R., DeGroott, J., Kiers, G. H., and van Weeren, P. R. (2004) Collagenase-1 (MMP-1) activity in equine synovial fluid: influence of age, joint pathology, exercise and repeated arthrocentesis, *Equine Vet J 36*, 34-40.
33. Brittberg, M., Lindahl, A., Nilsson, A., Ohlsson, C., Isaksson, O., and Peterson, L. (1994) Treatment of deep cartilage defects in the knee with autologous chondrocyte transplantation, *N Engl J Med 331*, 889-895.
34. Brommer, H., Brama, P. A., Laasanen, M. S., Helminen, H. J., van Weeren, P. R., and Jurvelin, J. S. (2005) Functional adaptation of articular cartilage from birth to maturity under the influence of loading: a biomechanical analysis, *Equine Vet J 37*, 148-154.
35. Brown, G. M., Huckerby, T. N., Bayliss, M. T., and Nieduszynski, I. A. (1998) Human aggrecan keratan sulfate undergoes structural changes during adolescent development, *J Biol Chem 273*, 26408-26414.

36. Buckwalter, J. A., and Mankin, H. J. (1997) Articular Cartilage, Part II: Degeneration and osteoarthrosis, repair, regeneration, and transplantation, *J Bone Joint Surg Am 79*, 612-632.
37. Buckwalter, J. A., and Martin, J. (1995) Degenerative joint disease, *Clin Symp 47*, 1-32.
38. Camacho, N., West, P., Yang, X., Lin, J., and Bostrom, M. (2002) An infrared fiber optic probe for detection of degenerative cartilage, *Trans Orthop Res Soc 27*, 225.
39. Camacho, N. P., West, P., Torzilli, P. A., and Mendelsohn, R. (2001) FTIR microscopic imaging of collagen and proteoglycan in bovine cartilage, *Biopolymers 62*, 1-8.
40. Carlson, C. S., Hilley, H. D., and Henrikson, C. K. (1985) Ultrastructure of normal epiphyseal cartilage of the articular-epiphyseal cartilage complex in growing swine, *Am J Vet Res 46*, 306-313.
41. Cawston, T. E., and Young, D. A. (2010) Proteinases involved in matrix turnover during cartilage and bone breakdown, *Cell Tissue Res 339*, 221-235.
42. Cheng, S., Kovanen, V., Heikkinen, E., and Suominen, H. (1996) Serum and urine markers of type I collagen metabolism in elderly women with high and low bone mineral density, *Eur J Clin Invest 26*, 186-191.
43. Clark, J. M., Norman, A., and Notzli, H. (1997) Postnatal development of the collagen matrix in rabbit tibial plateau articular cartilage, *J Anat 191*, 215-221.
44. Coats, A. M., Hukins, D. W., Imrie, C. T., and Aspden, R. M. (2003) Polarization artefacts of an FTIR microscope and the consequences for intensity measurements on anisotropic materials, *J Microsc 211*, 63-66.
45. Collett, E. (1992) *Polarized Light: Fundamentals and Applications*, Vol. 36, Mercel Dekker, New York.
46. Constantine, V. S., and Mowry, R. W. (1968) Selective staining of human dermal collagen. II. The use of picrosirius red F3BA with polarization microscopy, *J Invest Dermatol 50*, 419-423.

47. David-Vaudey, E., Burghardt, A., Keshari, K., Brouchet, A., Ries, M., and Majumdar, S. (2005) Fourier Transform Infrared Imaging of focal lesions in human osteoarthritic cartilage, *Eur Cell Mater 10*, 51-60; discussion 60.
48. Dayan, D., Hiss, Y., Hirshberg, A., Bubis, J. J., and Wolman, M. (1989) Are the polarization colors of picrosirius red-stained collagen determined only by the diameter of the fibers?, *Histochemistry 93*, 27-29.
49. DeGroot, J., Verzijl, N., Jacobs, K. M., Budde, M., Bank, R. A., Bijlsma, J. W., TeKoppele, J. M., and Lafeber, F. P. (2001) Accumulation of advanced glycation endproducts reduces chondrocyte-mediated extracellular matrix turnover in human articular cartilage, *Osteoarthritis Cartilage 9*, 720-726.
50. DeGroot, J., Verzijl, N., Wenting-Van Wijk, M. J., Bank, R. A., Lafeber, F. P., Bijlsma, J. W., and TeKoppele, J. M. (2001) Age-related decrease in susceptibility of human articular cartilage to matrix metalloproteinase-mediated degradation: the role of advanced glycation end products, *Arthritis rheum 44*, 2562-2571.
51. Dudhia, J. (2005) Aggrecan, aging and assembly in articular cartilage, *Cell Mol Life Sci 62*, 2241-2256.
52. Eikenberry, E. F., Mender, M., Bürgin, R., Winterhalter, K. H., and Bruckner, P. (1992) Fibrillar organization in cartilage, in *Articular cartilage and osteoarthrosis* (Kuettner, K., Ed.), pp 133-149, Raven Press, New York.
53. Erickson, S. J., Prost, R. W., and Timins, M. E. (1993) The "magic angle" effect: background physics and clinical relevance [editorial], *Radiology 188*, 23-25.
54. Eyre, D. (2002) Collagen of articular cartilage, *Arthritis Res 4*, 30-35.
55. Eyre, D. R., Paz, M. A., and Gallop, P. M. (1984) Cross-linking in collagen and elastin, *Annu Rev Biochem 53*, 717-748.
56. Eyre, D. R., Wu, J.-J., and Woods, P. (1992) Cartilage-Specific Collagens Structural Studies, in *Articular Cartilage and Osteoarthritis* (kuettner, K., Ed.), Raven Press, Ltd., New York.
57. Fabian, H., Lasch, P., Boese, M., and Haensch, W. (2002) Mid-IR microspectroscopic imaging of breast tumor tissue sections, *Biopolymers 67*, 354-357.

58. Fabian, H., Thi, N. A., Eiden, M., Lasch, P., Schmitt, J., and Naumann, D. (2006) Diagnosing benign and malignant lesions in breast tissue sections by using IR-microspectroscopy, *Biochim Biophys Acta 1758*, 874-882.
59. Fraser, R. D. M., and MacRae, T. P. (1973) *Conformation if fibrous proteins and related synthetic polypeptides*, Academic Press, New York.
60. Freeman, M. A. R., and Meachim, G. (1979) Ageing and degeneration, in *Adult articular cartilage* (Freeman, M. A. R., Ed.), Pitman Medical, Kent.
61. Fujimoto, D. (1980) Evidence for natural existence of pyridinoline crosslink in collagen, *Biochem Biophys Res Commun 93*, 948-953.
62. Geng, Y., McQuillan, D., and Roughley, P. J. (2006) SLRP interaction can protect collagen fibrils from cleavage by collagenases, *Matrix Biol 25*, 484-491.
63. Grunder, W. (2006) MRI assessment of cartilage ultrastructure, *NMR Biomed 19*, 855-876.
64. Grunder, W., Kanowski, M., Wagner, M., and Werner, A. (2000) Visualization of pressure distribution within loaded joint cartilage by application of angle-sensitive NMR microscopy, *Magn Reson Med 43*, 884-891.
65. Haapala, J., Arokoski, J. P. A., Hyttinen, M. M., Lammi, M., Tammi, M., Kovanen, V., Helminen, H. J., and Kiviranta, I. (1999) Remobilization does not fully restore immobilization induced articular cartilage atrophy, *Clin Orthop*, 218-229.
66. Hangody, L., and Fules, P. (2003) Autologous osteochondral mosaicplasty for the treatment of full-thickness defects of weight-bearing joints: ten years of experimental and clinical experience, *J Bone Joint Surg Am 85-A Suppl 2*, 25-32.
67. Hannila, I., Raina, S. S., Tervonen, O., Ojala, R., and Nieminen, M. T. (2009) Topographical variation of T2 relaxation time in the young adult knee cartilage at 1.5 T, *Osteoarthritis Cartilage 17*, 1570-1575.
68. Hardingham, T. E. (1979) The role of link-protein in the structure of cartilage proteoglycan aggregates, *Biochem J 177*, 237-247.

69. Hascall, V. C., and Sajdera, S. W. (1970) Physical properties and polydispersity of proteoglycan from bovine nasal cartilage, *J Biol Chem 245*, 4920-4930.
70. Hayes, W. C., Keer, L. M., Herrmann, G., and Mockros, L. F. (1972) A mathematical analysis for indentation tests of articular cartilage, *J Biomech 5*, 541-551.
71. Heinegård, D. K., and Pimental, E. R. (1992) Cartilage matrix proteins, in *Articular cartilage and osteoatrhritis* (Kuettner, K., Ed.), pp 95-111, Raven press, New York.
72. Helmick, C. G., Felson, D. T., Lawrence, R. C., Gabriel, S., Hirsch, R., Kwoh, C. K., Liang, M. H., Kremers, H. M., Mayes, M. D., Merkel, P. A., Pillemer, S. R., Reveille, J. D., and Stone, J. H. (2008) Estimates of the prevalence of arthritis and other rheumatic conditions in the United States. Part I, *Arthritis Rheum 58*, 15-25.
73. Helminen, H. J., Hyttinen, M. M., Lammi, M. J., Arokoski, J. P., Lapveteläinen, T., Jurvelin, J., Kiviranta, I., and Tammi, M. I. (2000) Regular joint loading in youth assists in the establishment and strengthening of the collagen network of articular cartilage and contributes to the prevention of osteoarthrosis later in life: a hypothesis, *J Bone Miner Metab 18*, 245-257.
74. Hunziker, E. B., Kapfinger, E., and Geiss, J. (2007) The structural architecture of adult mammalian articular cartilage evolves by a synchronized process of tissue resorption and neoformation during postnatal development, *Osteoarthritis Cartilage 15*, 403-413.
75. Hunziker, E. B., Michel, M., and Studer, D. (1997) Ultrastructure of adult human articular cartilage matrix after cryotechnical processing, *Microsc Res Tech 37*, 271-284.
76. Hyttinen, M. M., Holopainen, J., van Weeren, P. R., Firth, E. C., Helminen, H. J., and Brama, P. A. (2009) Changes in collagen fibril network organization and proteoglycan distribution in equine articular cartilage during maturation and growth, *J Anat 215*, 584-591.

77. Jackson, M., Choo, L. P., Watson, P. H., Halliday, W. C., and Mantsch, H. H. (1995) Beware of connective tissue proteins: assignment and implications of collagen absorptions in infrared spectra of human tissues, *Biochim Biophys Acta 1270*, 1-6.

78. Jackson, M., Sowa, M. G., and Mantsch, H. H. (1997) Infrared spectroscopy: a new frontier in medicine, *Biophys Chem 68*, 109-125.

79. Jadin, K. D., Wong, B. L., Bae, W. C., Li, K. W., Williamson, A. K., Schumacher, B. L., Price, J. H., and Sah, R. L. (2005) Depth-varying density and organization of chondrocytes in immature and mature bovine articular cartilage assessed by 3d imaging and analysis, *J Histochem Cytochem 53*, 1109-1119.

80. Jones, I. L., Larsson, S. E., and Lemperg, R. (1977) The glycosaminoglycans of human articular cartilage: concentration and distribution in different layers in the adult individual, *Clin Orthop 127*, 257-264.

81. Jortikka, M. O., Inkinen, R. I., Tammi, M. I., Parkkinen, J. J., Haapala, J., Kiviranta, I., Helminen, H. J., and Lammi, M. J. (1997) Immobilisation causes longlasting matrix changes both in the immobilised and contralateral joint cartilage, *Ann Rheum Dis 56*, 255-261.

82. Julkunen, P., Harjula, T., Iivarinen, J., Marjanen, J., Seppanen, K., Narhi, T., Arokoski, J., Lammi, M. J., Brama, P. A., Jurvelin, J. S., and Helminen, H. J. (2009) Biomechanical, biochemical and structural correlations in immature and mature rabbit articular cartilage, *Osteoarthritis Cartilage 17*, 1628-1638.

83. Julkunen, P., Kiviranta, P., Wilson, W., Jurvelin, J. S., and Korhonen, R. K. (2007) Characterization of articular cartilage by combining microscopic analysis with a fibril-reinforced finite-element model, *J Biomech 40*, 1862-1870.

84. Julkunen, P., Wilson, W., Jurvelin, J. S., Rieppo, J., Qu, C. J., Lammi, M. J., and Korhonen, R. K. (2008) Stress-relaxation of human patellar articular cartilage in unconfined compression: prediction of mechanical response by tissue composition and structure, *J Biomech 41*, 1978-1986.

85. Junqueira, L. C., Cossermelli, W., and Brentani, R. (1978) Differential staining of collagens type I, II and III by Sirius Red and polarization microscopy, *Arch Histol Jpn 41*, 267-274.
86. Junqueira, L. C., Montes, G. S., and Sanchez, E. M. (1982) The influence of tissue section thickness on the study of collagen by the Picrosirius-polarization method, *Histochemistry 74*, 153-156.
87. Junquiera, L. C., Junqueira, L. C., and Brentani, R. R. (1979) A simple and sensitive method for the quantitative estimation of collagen, *Anal Biochem 94*, 96-99.
88. Jurvelin, J., Kiviranta, I., Säämänen, A. M., Tammi, M., and Helminen, H. J. (1990) Indentation stiffness of young canine knee articular cartilage-- influence of strenuous joint loading, *J Biomech 23*, 1239-1246.
89. Jurvelin, J., Kiviranta, I., Tammi, M., and Helminen, H. J. (1986) Effect of physical exercise on indentation stiffness of articular cartilage in the canine knee, *Int J Sports Med 7*, 106-110.
90. Jurvelin, J. S., Buschmann, M. D., and Hunziker, E. B. (1997) Optical and mechanical determination of Poisson's ratio of adult bovine humeral articular cartilage, *J Biomech 30*, 235-241.
91. Kempson, G. E. (1991) Age-related changes in the tensile properties of human articular cartilage: a comparative study between the femoral head of the hip joint and the talus of the ankle joint, *Biochim Biophys Acta 1075*, 223-230.
92. Kempson, G. E. (1982) Relationship between the tensile properties of articular cartilage from the human knee and age, *Ann Rheum Dis 41*, 508-511.
93. Király, K., Hyttinen, M. M., Lapveteläinen, T., Elo, M., Kiviranta, I., Dobai, J., Modis, L., Helminen, H. J., and Arokoski, J. P. (1997) Specimen preparation and quantification of collagen birefringence in unstained sections of articular cartilage using image analysis and polarizing light microscopy, *Histochem J 29*, 317-327.
94. Kiviranta, I., Jurvelin, J., Tammi, M., Saamanen, A. M., and Helminen, H. J. (1985) Microspectrophotometric quantitation of glycosaminoglycans in articular cartilage sections stained with Safranin O, *Histochemistry 82*, 249-255.

95. Kiviranta, I., Tammi, M., Jurvelin, J., Säämänen, A. M., and Helminen, H. J. (1988) Moderate running exercise augments glycosaminoglycans and thickness of articular cartilage in the knee joint of young beagle dogs, *J Orthop Res 6*, 188-195.

96. Kiviranta, P., Rieppo, J., Korhonen, R. K., Julkunen, P., Töyräs, J., and Jurvelin, J. S. (2006) Collagen network primarily controls the Poisson's ratio of bovine articular cartilage in compression, *J Orthop Res 24*, 690-699.

97. Klein, T. J., Chaudhry, M., Bae, W. C., and Sah, R. L. (2007) Depth-dependent biomechanical and biochemical properties of fetal, newborn, and tissue-engineered articular cartilage, *J Biomech 40*, 182-190.

98. Kliger, D., and Lewis, J. (1990) *Polarized light in optics and spectroscopy*, Academic Press San Diego.

99. Knudson, C. B., and Knudson, W. (2001) Cartilage proteoglycans, *Semin Cell Dev Biol 12*, 69-78.

100. Kocsis, K., Hyttinen, M., Helminen, H. J., Aydelotte, M. B., and Modis, L. (1998) Combination of digital image analysis and polarization microscopy: theoretical considerations and experimental data, *Microsc Res Tech 43*, 511-517.

101. Kohler, A., Bertrand, D., Martens, H., Hannesson, K., Kirschner, C., and Ofstad, R. (2007) Multivariate image analysis of a set of FTIR microspectroscopy images of aged bovine muscle tissue combining image and design information, *Anal Bioanal Chem 389*, 1143-1153.

102. Kohler, A., Kirschner, C., Oust, A., and Martens, H. (2005) Extended multiplicative signal correction as a tool for separation and characterization of physical and chemical information in Fourier transform infrared microscopy images of cryo-sections of beef loin, *Appl Spectrosc 59*, 707-716.

103. Korhonen, R. K., Julkunen, P., Rieppo, J., Lappalainen, R., Konttinen, Y. T., and Jurvelin, J. S. (2006) Collagen network of articular cartilage modulates fluid flow and mechanical stresses in chondrocyte, *Biomechanics and Modeling in Mechanobiology 5*, 150-159.

104. Laasanen, M. S., Saarakkala, S., Toyras, J., Rieppo, J., and Jurvelin, J. S. (2005) Site-specific ultrasound reflection properties and superficial collagen content of bovine knee articular cartilage, *Phys Med Biol 50*, 3221-3233.
105. Lasch, P., Chiriboga, L., Yee, H., and Diem, M. (2002) Infrared spectroscopy of human cells and tissue: detection of disease, *Technol Cancer Res Treat 1*, 1-7.
106. Lasch, P., Diem, M., Hansch, W., and Naumann, D. (2007) Artificial neural networks as supervised techniques for FT-IR microspectroscopic imaging, *J Chemom 20*, 209-220.
107. Lasch, P., Haensch, W., Naumann, D., and Diem, M. (2004) Imaging of colorectal adenocarcinoma using FT-IR microspectroscopy and cluster analysis, *Biochim Biophys Acta 1688*, 176-186.
108. Lawrence, R. C., Felson, D. T., Helmick, C. G., Arnold, L. M., Choi, H., Deyo, R. A., Gabriel, S., Hirsch, R., Hochberg, M. C., Hunder, G. G., Jordan, J. M., Katz, J. N., Kremers, H. M., and Wolfe, F. (2008) Estimates of the prevalence of arthritis and other rheumatic conditions in the United States. Part II, *Arthritis Rheum 58*, 26-35.
109. Maroudas, A. (1968) Physicochemical properties of cartilage in the light of ion exchange theory, *Biophys J 8*, 575-595.
110. Maroudas, A., and Bannon, C. (1981) Measurement of swelling pressure in cartilage and comparison with the osmotic pressure of constituent proteoglycans, *Biorheology 18*, 619-632.
111. Maroudas, A., Evans, H., and Almeida, L. (1973) Cartilage of the hip joint. Topographical variation of glycosaminoglycan content in normal and fibrillated tissue, *Ann Rheum Dis 32*, 1-9.
112. Maroudas, A., Palla, G., and Gilav, E. (1992) Racemization of aspartic acid in human articular cartilage, *Connect Tissue Res 28*, 161-169.
113. Martel-Pelletier, J., Boileau, C., Pelletier, J. P., and Roughley, P. J. (2008) Cartilage in normal and osteoarthritis conditions, *Best Pract Res Clin Rheumatol 22*, 351-384.
114. Mayne, R. (1989) Cartilage collagens. What is their function, and are they involved in articular disease?, *Arthritis Rheum 32*, 241-246.

115. Meachim, G., and Stockwell, R. A. (1979) The matrix, in *Adult articular cartilage* (Freeman, M. A. R., Ed.), pp 1-50, Pitman Medical, Kent.
116. Miller, E. J. (1972) Structural studies on cartilage collagen employing limited cleavage and solubilization with pepsin, *Biochemistry 11*, 4903-4909.
117. Mitchell, D., and Hardingham, T. (1982) The control of chondroitin sulphate biosynthesis and its influence on the structure of cartilage proteoglycans, *Biochem J 202*, 387-395.
118. Modis, L. (1991) *Organization of the extracellular matrix: a polarization microscopic approach*, CRC Press, Boca Raton.
119. Mok, M. T., Ilic, M. Z., Handley, C. J., and Robinson, H. C. (1992) Cleavage of proteoglycan aggregate by leucocyte elastase, *Arch Biochem Biophys 292*, 442-447.
120. Moore, A. R., Appelboam, A., Kawabata, K., Da Silva, J. A., D'Cruz, D., Gowland, G., and Willoughby, D. A. (1999) Destruction of articular cartilage by alpha 2 macroglobulin elastase complexes: role in rheumatoid arthritis, *Ann Rheum Dis 58*, 109-113.
121. Mow, V. C., Fithian, D. C., and Kelly, M. A. (1990) Fundamentals of articular cartilage and meniscus biomechanics, in *Articular cartilage and knee joint function: basic science and arthroscopy* (Ewing, J. W., Ed.), pp 1-18, Raven Press Ltd., New York.
122. Muir, H. (1980) The chemistry of the ground substance of joint cartilage, in *The joints and synovial fluid* (Sokoloff, L., Ed.), pp 27-94, Academic Press, New York.
123. Nakano, T., Aherne, F. X., and Thompson, J. R. (1978) Changes in swine knee articular cartilage during growth, *Can J Anim Sci 59*, 167-179.
124. Newman, A. P. (1998) Articular cartilage repair, *American Journal of Sports Medicine 26*, 309-324.
125. Nieminen, H. J., Töyräs, J., Rieppo, J., Nieminen, M. T., Hirvonen, J., Korhonen, R., and Jurvelin, J. S. (2002) Real-time ultrasound analysis of articular cartilage degradation in vitro, *Ultrasound Med Biol 28*, 519-525.

126. Nieminen, M. T., Rieppo, J., Silvennoinen, J., Toyras, J., Hakumaki, J. M., Hyttinen, M. M., Helminen, H. J., and Jurvelin, J. S. (2002) Spatial assessment of articular cartilage proteoglycans with Gd-DTPA-enhanced T1 imaging, *Magn Reson Med 48*, 640-648.
127. Nieminen, M. T., Rieppo, J., Töyräs, J., Hakumäki, J. M., Silvennoinen, M. J., Hyttinen, M. M., Helminen, H. J., and Jurvelin, J. S. (2001) T2 relaxation reveals spatial collagen architecture in articular cartilage: a comparative quantitative MRI and polarized light microscopic study, *Magn Reson Med 46*, 487-493.
128. Nieminen, M. T., Toyras, J., Rieppo, J., Hakumaki, J. M., Silvennoinen, J., Helminen, H. J., and Jurvelin, J. S. (2000) Quantitative MR microscopy of enzymatically degraded articular cartilage, *Magn Reson Med 43*, 676-681.
129. Nissi, M. J., Rieppo, J., Toyras, J., Laasanen, M. S., Kiviranta, I., Jurvelin, J. S., and Nieminen, M. T. (2006) T(2) relaxation time mapping reveals age- and species-related diversity of collagen network architecture in articular cartilage, *Osteoarthritis Cartilage 14*, 1265-1271.
130. Nissi, M. J., Toyras, J., Laasanen, M. S., Rieppo, J., Saarakkala, S., Lappalainen, R., Jurvelin, J. S., and Nieminen, M. T. (2004) Proteoglycan and collagen sensitive MRI evaluation of normal and degenerated articular cartilage, *J Orthop Res 22*, 557-564.
131. Närhi, T., Rieppo, L., Saarakkala, S., Jurvelin, J. S., Helminen, H. J., and Rieppo, J. (2010) Increased Specificity for Measurement of the Spatial Distribution of Articular Cartilage Proteoglycans with Fourier Transform Infrared Imaging Spectroscopy: Application of Second Derivative Spectroscopy and Principal Component Noise Reduction Techniques, *unpublished manuscript*.
132. Oldenbourg, R. (1996) A new view on polarization microscopy, *Nature 381*, 811-812.
133. Oldenbourg, R. (2008) Polarized light field microscopy: an analytical method using a microlens array to simultaneously capture both conoscopic and orthoscopic views of birefringent objects, *J Microsc 231*, 419-432.

134. Oldenbourg, R., and Mei, G. (1995) New polarized light microscope with precision universal compensator, *J Microsc 180*, 140-147.
135. Ortmann, R. (1975) Use of polarized light for quantitative determination of the adjustment of the tangential fibres in articular cartilage, *Anat Embryol (Berl) 148*, 109-120.
136. Pal, S., Tang, L. H., Choi, H., Habermann, E., Rosenberg, L., Roughley, P., and Poole, A. R. (1981) Structural changes during development in bovine fetal epiphyseal cartilage, *Coll Relat Res 1*, 151-176.
137. Palokangas, H., Kovanen, V., Duncan, A., and Robins, S. P. (1992) Age-related changes in the concentration of hydroxypyridinium crosslinks in functionally different skeletal muscles, *Matrix 12*, 291-296.
138. Paschalis, E. P., Betts, F., DiCarlo, E., Mendelsohn, R., and Boskey, A. L. (1997) FTIR microspectroscopic analysis of human iliac crest biopsies from untreated osteoporotic bone, *Calcif Tissue Int 61*, 487-492.
139. Paukkonen, K., and Helminen, H. J. (1987) Decrease of proteoglycan granule number but increase of their size in articular cartilage of young rabbits after physical exercise and immobilization by splinting, *Anat Rec 219*, 45-52.
140. Potter, K., Kidder, L. H., Levin, I. W., Lewis, E. N., and Spencer, R. G. (2001) Imaging of collagen and proteoglycan in cartilage sections using Fourier transform infrared spectral imaging, *Arthritis Rheum 44*, 846-855.
141. Puchtler, H., Meloan, S. N., and Waldrop, F. S. (1988) Are picro-dye reactions for collagens quantitative? Chemical and histochemical considerations, *Histochemistry 88*, 243-256.
142. Puchtler, H., Waldrop, F. S., and Valentine, L. S. (1973) Polarization microscopic studies of connective tissue stained with picro-sirius red FBA, *Beitr Pathol 150*, 174-187.
143. Radin, E. L. (1998) The aetiology and treatment of osteoarthrosis and how to elucidate them, *Rheumatology in Europe 27*, 47-48.
144. Radin, E. L., Paul, I. L., and Tolkoff, M. J. (1970) Subchondral bone changes in patients with early degenerative joint disease, *Arthritis Rheum 13*, 400-405.

145. Ramakrishnan, N., Xia, Y., and Bidthanapally, A. (2008) Fourier-transform infrared anisotropy in cross and parallel sections of tendon and articular cartilage, *J Orthop Surg 3*, 48.
146. Ramakrishnan, N., Xia, Y., and Bidthanapally, A. (2007) Polarized IR microscopic imaging of articular cartilage, *Phys Med Biol 52*, 4601-4614.
147. Ramakrishnan, N., Xia, Y., Bidthanapally, A., and Lu, M. (2007) Determination of zonal boundaries in articular cartilage using infrared dichroism, *Appl Spectrosc 61*, 1404-1409.
148. Ratcliffe, A., Fryer, P. R., and Hardingham, T. E. (1984) The distribution of aggregating proteoglycans in articular cartilage: comparison of quantitative immunoelectron microscopy with radioimmunoassay and biochemical analysis, *J Histochem Cytochem 32*, 193-201.
149. Rieppo, J., Rieppo, L., Hyttinen, M. M., Jurvelin, J. S., Kiviranta, I., and Helminen, H. J. (2007) Characterization of hte Articular Cartilage Repair Tissue with Fourier Transform Infrared Imaging Spectroscopy and Cluster Analysis, *Transact Orthop Res Soc 32*, 666.
150. Rieppo, L., Saarakkala, S., Narhi, T., Holopainen, J., Lammi, M., Helminen, H. J., Jurvelin, J. S., and Rieppo, J. (2010a) Quantitative analysis of spatial proteoglycan content in articular cartilage with Fourier transform infrared imaging spectroscopy: Critical evaluation of analysis methods and specificity of the parameters, *Microsc Res Tech 73*, 503-512.
151. Rieppo, L., Saarakkala, S., Närhi, T., Holopainen, J., Lammi, M., Helminen, H. J., Jurvelin, J. S., and Rieppo, J. (2010b) Increased Molecular Specificity for Fourier Transform Infrared Imaging Spectroscopy of Articular Cartilage: Application of Second Derivative Spectroscopy, *unpublished manuscript*.
152. Roth, V., and Mow, V. C. (1980) The intrinsic tensile behavior of the matrix of bovine articular cartilage and its variation with age, *J Bone Joint Surg Am 62*, 1102-1117.
153. Rubenstein, J. D., Kim, J. K., Morova-Protzner, I., Stanchev, P. L., and Henkelman, R. M. (1993) Effects of collagen orientation on MR imaging characteristics of bovine articular cartilage, *Radiology 188*, 219-226.

154. Saarakkala, S., Julkunen, P., Kiviranta, P., Makitalo, J., Jurvelin, J. S., and Korhonen, R. K. (2009) Depth-wise progression of osteoarthritis in human articular cartilage: investigation of composition, structure and biomechanics, *Osteoarthritis Cartilage 18*, 73-81.
155. Sahu, R. K., and Mordechai, S. (2005) Fourier transform infrared spectroscopy in cancer detection, *Future Oncol 1*, 635-647.
156. Santer, V., White, R. J., and Roughley, P. J. (1982) O-Linked oligosaccharides of human articular cartilage proteoglycan, *Biochim Biophys Acta 716*, 277-282.
157. Schenk, R. K., Eggli, P. S., and Hunziker, E. B. (1986) Articular cartilage morphology, in *Articular cartilage biochemistry* (Kuettner, K. E., Ed.), pp 3-22, Raven Press, New York.
158. Servaty, R., Schiller, J., Binder, H., and Arnold, K. (2001) Hydration of Polymeric Components of Cartilage- An Infrared Study on Hyaluronic Acid and Chondroitin Sulphate., *Int J Biol Macromol 28*, 121-127.
159. Service, R. F. (2008) Tissue engineering. Coming soon to a knee near you: cartilage like your very own, *Science 322*, 1460-1461.
160. Shingleton, W. D., Hodges, D. J., Brick, P., and Cawston, T. E. (1996) Collagenase: a key enzyme in collagen turnover, *Biochem Cell Biol 74*, 759-775.
161. Speer, D. P., and Dahners, L. (1979) The collagenous architecture of articular cartilage. Correlation of scanning electron microscopy and polarized light microscopy observations, *Clin Orthop*, 267-275.
162. Strider, W., Pal, S., and Rosenberg, L. (1975) Comparison of proteoglycans from bovine articular cartilage, *Biochim Biophys Acta 379*, 271-281.
163. Stuart, B. (2004) *Infrared spectroscopy: Fundamentals and applications*, Wiley, Chichester.
164. Suh, J. K., Li, Z., and Woo, S. L. (1995) Dynamic behavior of a biphasic cartilage model under cyclic compressive loading, *J Biomech 28*, 357-364.

165. Tammi, R. H., Tammi, M. I., Hascall, V. C., Hogg, M., Pasonen, S., and MacCallum, D. K. (2000) A preformed basal lamina alters the metabolism and distribution of hyaluronan in epidermal keratinocyte "organotypic" cultures grown on collagen matrices, *Histochem Cell Biol 113*, 265-277.
166. Tang, L. H., Buckwalter, J. A., and Rosenberg, L. C. (1996) Effect of link protein concentration on articular cartilage proteoglycan aggregation, *J Orthop Res 14*, 334-339.
167. Thonar, E. J., and Sweet, M. B. (1981) Maturation-related changes in proteoglycans of fetal articular cartilage, *Arch Biochem Biophys 208*, 535-547.
168. Töyräs, J., Rieppo, J., Nieminen, M. T., Helminen, H. J., and Jurvelin, J. S. (1999) Characterization of enzymatically induced degradation of articular cartilage using high frequency ultrasound, *Phys Med Biol 44*, 2723-2733.
169. van Turnhout, M. C., Kranenbarg, S., and van Leeuwen, J. L. (2010b) Contribution of postnatal collagen reorientation to depth-dependent mechanical properties of articular cartilage, *Biomech Model Mechanobiol*.
170. van Turnhout, M. C., Schipper, H., Engel, B., Buist, W., Kranenbarg, S., and van Leeuwen, J. L. (2010a) Postnatal development of collagen structure in ovine articular cartilage, *BMC Dev Biol 10*, 62.
171. van Weeren, P. R., Firth, E. C., Brommer, B., Hyttinen, M. M., Helminen, A. E., Rogers, C. W., Degroot, J., and Brama, P. A. (2008) Early exercise advances the maturation of glycosaminoglycans and collagen in the extracellular matrix of articular cartilage in the horse, *Equine Vet J 40*, 128-135.
172. Wang, X., Liang, J., Koike, T., Sun, H., Ichikawa, T., Kitajima, S., Morimoto, M., Shikama, H., Watanabe, T., Sasaguri, Y., and Fan, J. (2004) Overexpression of human matrix metalloproteinase-12 enhances the development of inflammatory arthritis in transgenic rabbits, *Am J Pathol 165*, 1375-1383.

173. Vasara, A. I., Hyttinen, M. M., Pulliainen, O., Lammi, M. J., Jurvelin, J. S., Peterson, L., Lindahl, A., Helminen, H. J., and Kiviranta, I. (2006) Immature porcine knee cartilage lesions show good healing with or without autologous chondrocyte transplantation, *Osteoarthritis Cartilage 14*, 1066-1074.
174. Wei, X., Räsänen, T., and Messner, K. (1998) Maturation-related compressive properties of rabbit knee articular cartilage and volume fraction of subchondral tissue, *Osteoarthritis Cartilage 6*, 400-409.
175. Venn, M., and Maroudas, A. (1977) Chemical composition and swelling of normal and osteoarthrotic femoral head cartilage. I. Chemical composition, *Ann Rheum Dis 36*, 121-129.
176. Verzijl, N., DeGroot, J., Thorpe, S. R., Bank, R. A., Shaw, J. N., Lyons, T. J., Bijlsma, J. W., Lafeber, F. P., Baynes, J. W., and TeKoppele, J. M. (2000) Effect of collagen turnover on the accumulation of advanced glycation end products, *J Biol Chem 275*, 39027-39031.
177. Vesela, A., Barros, A. S., Synytsya, A., Delgadillo, I., Copikova, J., and Coimbra, M. A. (2007) Infrared spectroscopy and outer product analysis for quantification of fat, nitrogen, and moisture of cocoa powder, *Anal Chim Acta 601*, 77-86.
178. West, P. A., Bostrom, M. P., Torzilli, P. A., and Camacho, N. P. (2004) Fourier transform infrared spectral analysis of degenerative cartilage: an infrared fiber optic probe and imaging study, *Appl Spectrosc 58*, 376-381.
179. West, P. A., Torzilli, P. A., Chen, C., Lin, P., and Camacho, N. P. (2005) Fourier transform infrared imaging spectroscopy analysis of collagenase-induced cartilage degradation, *J Biomed Opt 10*, 14015.
180. Williamson, A. K., Chen, A. C., Masuda, K., Thonar, E. J., and Sah, R. L. (2003) Tensile mechanical properties of bovine articular cartilage: variations with growth and relationships to collagen network components, *J Orthop Res 21*, 872-880.
181. Williamson, A. K., Chen, A. C., and Sah, R. L. (2001) Compressive properties and function-composition relationships of developing bovine articular cartilage, *J Orthop Res 19*, 1113-1121.

182. Williamson, A. K., Masuda, K., Thonar, E. J., and Sah, R. L. (2003) Growth of immature articular cartilage in vitro: correlated variation in tensile biomechanical and collagen network properties, *Tissue Eng 9*, 625-634.
183. Xia, Y. (2000) Heterogeneity of cartilage laminae in MR imaging, *J Magn Reson Imaging 11*, 686-693.
184. Xia, Y., Alhadlaq, H., Ramakrishnan, N., Bidthanapally, A., Badar, F., and Lu, M. (2008) Molecular and morphological adaptations in compressed articular cartilage by polarized light microscopy and Fourier-transform infrared imaging, *J Struct Biol 164*, 88-95.
185. Xia, Y., Moody, J. B., Alhadlaq, H., Burton-Wurster, N., and Lust, G. (2002) Characteristics of topographical heterogeneity of articular cartilage over the joint surface of a humeral head, *Osteoarthritis Cartilage 10*, 370-380.
186. Xia, Y., Moody, J. B., Alhadlaq, H., and Hu, J. (2003) Imaging the physical and morphological properties of a multi-zone young articular cartilage at microscopic resolution, *J Magn Reson Imaging 17*, 365-374.
187. Xia, Y., Moody, J. B., Burton-Wurster, N., and Lust, G. (2001) Quantitative in situ correlation between microscopic MRI and polarized light microscopy studies of articular cartilage, *Osteoarthritis Cartilage 9*, 393-406.
188. Xia, Y., Ramakrishnan, N., and Bidthanapally, A. (2007) The depth-dependent anisotropy of articular cartilage by Fourier-transform infrared imaging (FTIRI), *Osteoarthritis Cartilage 15*, 780-788.
189. Yamagata, T., Saito, H., Habuchi, O., and Suzuki, S. (1968) Purification and properties of bacterial chondroitinases and chondrosulfatases, *J Biol Chem 243*, 1523-1535.

Jarno Rieppo

Microscopic and Spectroscopic Analysis of Immature and Mature Articular Cartilage

Postnatal changes in collagen network during articular cartilage (AC) maturation have been unknown. This study aimed at developing the existing microscopic and spectroscopic techniques capable of detailed characterization of AC. Thesis work proved that imaging techniques are able to reveal local tissue changes earlier than traditional biochemical methods. The results also demonstrated that AC undergoes significant alterations during maturation. These findings support the hypothesis that physical exercise during childhood may strengthen the collagen network and prevent osteoarthrosis in adulthood.

UNIVERSITY OF
EASTERN FINLAND

Publications of the University of Eastern Finland
Dissertations in Health Sciences

ISBN 978-952-61-0355-6